# A membrane-depolarising toxin substrate of the *Staphylococcus aureus* Type VII protein secretion system targets eukaryotes and bacteria

Fatima R. Ulhuq[1], Gina Duggan[2,3], Manman Guo[4], Chriselle Mendonca[1,5], James D. Chalmers[1,6], Zhenping Cao[1], Holger Kneuper[1], Sarah Murdoch[1], Sarah Thomson[7], Henrik Strahl[5], Matthias Trost[4,8], Serge Mostowy[2,3] and Tracy Palmer[1,5†]

[1]Division of Molecular Microbiology, School of Life Sciences, University of Dundee, Dundee DD1 5EH, UK

[2]Section of Microbiology, MRC Centre for Molecular Bacteriology and Infection, Imperial College London, Armstrong Road, London SW7 2AZ, UK

[3]Department of Immunology & Infection, London School of Hygiene & Tropical Medicine, Keppel Street, London WC1E 7HT, UK

[4]MRC Protein Phosphorylation and Ubiquitylation Unit, School of Life Sciences, University of Dundee, Dundee DD1 5EH, UK

[5]Centre for Bacterial Cell Biology, Institute for Cell and Molecular Biosciences, Newcastle University, Newcastle upon Tyne, NE2 4HH, UK

[6]Division of Molecular and Clinical Medicine, University of Dundee, Dundee, DD1 9SY, UK

[7]Biological Services, School of Life Sciences, University of Dundee, Dundee DD1 5EH, UK

[8]Institute for Cell and Molecular Biosciences, Newcastle University, Newcastle-upon-Tyne

[†]for correspondence tracy.palmer@newcastle.ac.uk

**Summary**

The type VII protein secretion system (T7SS) is conserved across *Staphylococcus aureus* strains and plays important roles in virulence and interbacterial competition. To date only one T7SS substrate protein, encoded in a subset of strains, has been functionally characterized. Here, using an unbiased proteomic approach, we identify TspA as a further T7SS substrate. TspA, encoded distantly from the T7SS gene cluster, is found across all *S. aureus* strains. Heterologous expression of TspA indicates that it has a toxic C-terminal domain that depolarizes membranes. The membrane depolarizing activity is alleviated by co-production of the TsaI immunity protein. Using a zebrafish hindbrain ventricle infection model, we demonstrate that the T7SS of strain RN6390 contributes to zebrafish mortality, and deletion of *tspA* leads to increased bacterial clearance *in vivo*. The toxin domain of TspA is highly polymorphic and *S. aureus* strains encode multiple *tsaI* homologues at the *tspA* locus, suggestive of additional roles in intra-species competition. In agreement, we demonstrate TspA-dependent growth inhibition of RN6390 by strain COL in the zebrafish infection model, that is alleviated by the presence of TsaI homologues. This is the first T7SS substrate protein shown to have activity against both eukaryotes and prokaryotes.

43 **Introduction**

44 The Type VII secretion system (T7SS) has been characterised in bacteria of the actinobacteria
45 and firmicutes phyla. In pathogenic mycobacteria the ESX-1 T7SS secretes numerous
46 proteins that are essential for virulence and immune evasion[1]. The Ess T7SS of
47 *Staphylococcus aureus* is also required for pathogenesis in murine models of infection[2, 3, 4],
48 and a longitudinal study of persistent *S. aureus* infection in the airways of a cystic fibrosis
49 patient showed that the *ess* T7SS genes were highly upregulated during a 13 year timespan[5].
50 It is becoming increasingly apparent, however, that in addition to having anti-eukaryotic
51 activity, the T7SS of firmicutes mediates interbacterial competition[6, 7, 8]. Some strains of *S.*
52 *aureus* secrete a DNA endonuclease toxin, EsaD[6, 9], that when overproduced leads to growth
53 inhibition of a sensitive *S. aureus* strain[6]. Moreover, *Streptococcus intermedius* exports at
54 least three LXG domain-containing toxins, TelA, TelB and TelC that mediate contact-
55 dependent growth inhibition against a range of Gram positive species[7].

56 A large integral membrane ATPase of the FtsK/SpoIIIE family, termed EssC in firmicutes, is a
57 conserved component of all T7SSs and probably energizes protein secretion as well as
58 forming part of the translocation channel[10, 11, 12, 13]. Three further membrane proteins function
59 alongside the ATPase to mediate T7 protein secretion[2, 3, 13, 14, 15]. EsxA, a small secreted
60 protein of the WXG100 family, is a further conserved T7 component that is dependent on the
61 T7SS for its translocation across the membrane[2, 16]. In *S. aureus* the T7 structural components
62 are encoded at the *ess* locus. In commonly-studied *S. aureus* strains including Newman,
63 RN6390 and USA300, the T7 substrates EsxB, EsxC, EsxD and EsaD are encoded
64 immediately downstream of *essC* (Fig 1A) and are co-regulated with the genes coding for
65 machinery components[2, 3, 6, 9, 17, 18]. With the exception of EsaD the biological activities of these
66 substrates are unknown, although mutational studies have suggested that EsxB and EsxC
67 contribute to persistent infection in a murine abscess model[2, 17].

68 Despite the *ess* locus forming part of the core *S. aureus* genome, these four substrate proteins
69 are not conserved across *S. aureus* isolates, being found in only approximately 50% of
70 sequenced strains[19]. Furthermore, inactivation of the T7SS in *S. aureus* strain ST398 shows

71 a similar decrease in kidney abscess formation as that seen for T7 mutants in Newman and
72 USA300[2, 4, 20], despite the fact that recognizable homologues of EsxB/EsxC/EsxD/EsaD are
73 not encoded by this strain[19]. This strongly suggests that there are further *S. aureus* T7
74 substrates that are yet to be identified. Here we have taken an unbiased approach to identify
75 T7 substrates using quantitative proteomic analysis of culture supernatants from *S. aureus*
76 RN6390 wild type and *essC* strains. We identify a new substrate, TspA that is encoded
77 distantly from the *ess* gene cluster and is found in all sequenced *S. aureus* strains. Further
78 analysis indicates that TspA has a toxic C-terminal domain that depolarizes membranes.
79 Using a zebrafish hindbrain ventricle infection model, we reveal that TspA is important for
80 zebrafish killing and interbacterial competition *in vivo*.

81 **Results**

82 **The *S. aureus* RN6390 T7SS secreted proteome**

83 To identify candidate T7 substrates, RN6390 and an isogenic *essC* deletion strain[3] were
84 cultured in the minimal medium RPMI. Both strains grew identically (Fig 1B) and expressed
85 components of the T7SS, and as expected secretion of EsxA was abolished in the *essC* strain
86 (Fig 1C). Culture supernatants were isolated when cells reached $OD_{600nm}$ of 1, and label-free
87 quantitative proteomics used to assess changes in protein abundance of four biological
88 replicates of each secretome. Following identification of 1170 proteins, 17 proteins showed,
89 with high confidence ($p < 0.05$, 2-fold change), a decrease in abundance in the secretome of
90 the *essC* strain relative to the RN6390 parent strain (Fig 1D, Fig 1E; Table S1).

91 Proteomic analysis indicated that the secreted core component, EsxA, was significantly
92 reduced in abundance in the *essC* secretome, as expected from the western blot analysis (Fig
93 1C). Peptides from the membrane-bound T7 component EsaA, which has a large surface-
94 exposed loop[21], were also less abundant in the supernatant of the *essC* strain, as were EsxD
95 and EsaD, known substrates of the T7SS[6, 9, 18] (Table 1, Table S1). The EsxC substrate[17] was
96 also exclusively detected in the supernatant of the wild type strain, but only two EsxC peptides
97 were detected and it did not meet the $p < 0.01$ cut-off (Table S1). EsxB, another previously
98 identified substrate[2, 22], and EsaE, which is co-secreted with EsaD[6] were not detected in any
99 of our analysis.

100 After EsxD, the protein with the highest relative abundance in the secretome of the wild type
101 strain was the uncharacterized protein SAOUHSC_00584. This protein harbours a predicted
102 LXG domain which is common to some T7SS substrates[7]. Other proteins enriched in the
103 secretome of the wild type strain include a predicted superantigen (SAOUHSC_00389), the
104 secretory antigen SsaA, two predicted membrane-bound lipoproteins (SAOUHSC_01180 and
105 SAOUHSC_02695), two uncharacterized proteins (SAOUHSC_00406 and
106 SAOUHSC_02448) and several predicted cytoplasmic proteins (Table 1). A small number of

107 proteins were found to be enriched in abundance in the *essC* secretome (Table S1), including
108 the heme oxygenase IsdI, which is known to be upregulated when the T7SS is inactivated[23].

109

110 **SAOUHSC_00584/TspA localizes to the membrane dependent on EssC**

111 We next constructed tagged variants of each of SAOUHSC_00389, SAOUHSC_00406,
112 SAOUHSC_00584, SAOUHSC_02448 and SsaA to probe their subcellular locations in the
113 wild type and Δ*essC* strains. C-terminally HA-tagged SAOUHSC_00389, SAOUHSC_02448
114 and SsaA were secreted into the culture supernatant in an *essC*-independent manner (Fig
115 S1), indicating that these proteins are not substrates of the T7SS and their reduced abundance
116 in the *essC* secretome may arise for pleiotropic reasons. Overproduction of C-terminally Myc-
117 tagged SAOUHSC_00406 caused cell lysis, seen by the presence of TrxA in the supernatant
118 samples (Fig S1B). By contrast, a C-terminally Myc-tagged variant of SAOUHSC_00584 was
119 detected only in the cellular fraction (Fig S1C). To probe the subcellular location of
120 SAOUHSC_00584-Myc, we generated cell wall, membrane and cytoplasmic fractions. Fig 2A
121 shows that the tagged protein localizes to the membrane and that it appears to be destabilized
122 by the loss of EssC. SAOUHSC_00584 was subsequently renamed TspA (Type Seven
123 dependent Protein A).

124 TspA is predicted to be 469 amino acids long and to have either one (TMHMM) or two
125 (Predictprotein.org) transmembrane domains towards its C-terminal end. To determine
126 whether it is an integral membrane protein we washed isolated membranes with urea which
127 removes peripherally bound proteins by denaturation. Fig 2B indicates that a large fraction of
128 TspA-Myc is displaced from the membrane to the cytoplasmic fraction by urea whereas a *bona*
129 *fide* integral membrane protein, EssB, is not displaced by this treatment[24, 25, 26]. We conclude
130 that TspA-Myc peripherally interacts with the membrane. This is consistent with findings from
131 the proteomic experiment as peptides along the entire length of TspA were detected in the
132 secretome (Fig S2).

133 To determine whether TspA-Myc is exposed at the extracellular side we prepared
134 spheroplasts and treated them with proteinase K. Fig 2C shows that at low concentrations of
135 proteinase K, TspA-Myc was proteolytically cleaved to release a smaller fragment that also
136 cross-reacted with the anti-Myc antibody. At least part of this smaller fragment must be
137 extracellular as it was also degraded as the protease concentration was increased. An
138 approximately 37 kDa C-terminal fragment of TspA-Myc detected natively in the absence of
139 added protease was also extracellular as it was sensitive to digestion by proteinase K. The
140 likely topology of TspA is shown in Fig 2E.

141 All *S. aureus* T7SS substrate proteins identified to date are found only in a subset of strains,
142 and are linked with specific *essC* subtypes. However, TspA is encoded by all *S. aureus*
143 genomes examined in[19], and is distant from the *ess* locus. This raised the possibility that TspA
144 may be a further secreted core component of the T7 machinery. To examine this, we
145 constructed an in-frame *tspA* deletion in RN6390 and investigated the subcellular location of
146 the T7 secreted component EsxA and the substrate protein EsxC. Fig 2D shows that both
147 EsxA and EsxC are secreted in the absence of TspA. We conclude that TspA is a peripheral
148 membrane protein substrate of the T7SS whose localization and/or stability at the extracellular
149 side of the membrane is dependent on EssC, and that it is not a core component of the T7SS.

150

151 **TspA has a toxic C-terminal domain with membrane depolarizing activity that is**
152 **neutralized by TsaI**

153 Sequence analysis of TspA indicates that homologues are found across the *Staphylococci*
154 (including *S. argenteus*, *S. epidermidis* and *S. lugdunensis*), in *Listeria* species and
155 Enterococci, but does not provide clues about potential function. However, analysis of TspA
156 using modelling programs predicts strong structural similarity to colicin Ia (Fig 3A), a
157 bactericidal protein produced by some strains of *Escherichia coli*. Colicin Ia has an
158 amphipathic domain at its C-terminus that inserts into the cytoplasmic membrane from the

159 extracellular side to form a voltage-gated channel[27, 28, 29]. To investigate the function of TspA,
160 DNA encoding full length TspA or the C-terminal domain alone ($TspA_{CT}$) was cloned into a
161 tightly-regulatable vector for expression in *E. coli*. Fig 3C shows that production of TspA or
162 $TspA_{CT}$ did not affect *E. coli* survival. However, colicin Ia shows a sidedness for channel
163 formation because it requires a transmembrane voltage for full insertion[30]. We therefore
164 targeted $TspA_{CT}$ to the periplasm of *E. coli* by fusing to a Tat signal peptide[31, 32]. Fig 3C shows
165 that this construct was toxic, and that toxicity was relieved when the Tat pathway was
166 inactivated (Fig 3C), consistent with the C-terminal domain of TspA exerting toxic activity from
167 the periplasmic side of the membrane.

168 To assess $TspA_{CT}$ activity we first used the BacLight assay to test for membrane
169 depolarization. This uses 3,3′-diethyloxacarbocyanine iodide $DiOC_2(3)$, a dye that exhibits
170 green florescence in dilute solution but a red shift following membrane potential-driven
171 accumulation in the bacterial cytosol. After sorting of *E. coli* cells by flow cytometry it was seen
172 that the majority of *E. coli* cells harbouring the empty vector exhibited red fluorescence, which
173 shifted to green following treatment with the uncoupler carbonyl cyanide 3-
174 chlorophenylhydrazone (CCCP). A similar shift in fluorescence was also observed when *E.*
175 *coli* produced the AmiAss-$TspA_{CT}$ fusion (Fig 3D), indicative of loss of membrane potential.
176 We conclude that the C-terminal domain of TspA has membrane depolarising activity.

177 Pore-forming proteins are widely used as toxins to target either prokaryotic or eukaryotic
178 cells[33, 34]. To determine whether TspA forms pores we used single-cell microscopy that
179 combines the voltage-sensitive dye $DiSC_3(5)$ with the membrane-impermeable nucleic acid
180 stain Sytox Green[35]. *E. coli* cells incubated with Polymyxin B, which produces large ion-
181 permeable pores in the *E. coli* cell envelope[36], showed strong labelling with Sytox Green,
182 indicative of permeabilisation, coupled with very low $DiSC_3$ fluorescence (Fig 3E-G). By
183 contrast, cells harbouring the empty vector had high $DiSC_3$ fluorescence that was unaffected
184 by supplementation with the inducer L-arabinose, and did not stain with Sytox Green. Cells
185 expressing the AmiAss-$TspA_{CT}$ fusion following incubation with arabinose rapidly depolarised,

186 as evidenced by the marked reduction in $DiSC_3$ fluorescence, but did not detectably stain with
187 Sytox Green, even after prolonged periods of incubation (Fig 3E-G, Fig S3). Therefore, it
188 appears that TspA acts by triggering membrane depolarisation but does so by forming ion
189 channels rather than larger, nonselective pores in the *E. coli* inner membrane.

190 Bacterially-produced channel-forming toxins are often co-expressed with immunity proteins
191 that protect the producing cell from self-intoxication; for example, protection from colicin Ia
192 toxicity is mediated by the membrane-bound Iia immunity protein[37]. TspA is genetically linked
193 to a repeat region of ten genes encoding predicted polytopic membrane proteins with DUF443
194 domains (Fig 3B). To assess whether the DUF443-domain protein encoded adjacent to TspA
195 offers protection against the toxicity of the TspA C-terminal domain, we co-produced the
196 AmiAss-$TspA_{CT}$ fusion alongside SAOUHSC_00585 in *E. coli*. Fig 3C shows that co-
197 production of SAOUHSC_00585 offered protection of *E. coli* (Fig 3C). It also protected cells
198 from AmiAss-$TspA_{CT}$-induced depolarisation (Fig 3D-G). SAOUHSC_00585 was
199 subsequently renamed TsaI (TspA Immunity protein).

200

201 **A zebrafish model for *S. aureus* infection and T7SS activity.**

202 To probe whether TspA is important for *S. aureus* virulence, we initially developed an
203 immunocompetent murine model of *S. aureus* pneumonia. Previous reports have indicated
204 that 2-4 x $10^8$ colony forming units (cfu) of strain Newman was a suitable infectious dose, and
205 that bacterial proliferation in lung tissue could be observed after 24 hours[38]. We found that at
206 a dose of 8 x $10^7$ – 2 x $10^8$ of strain RN6390, the mice were asymptomatic and had almost
207 completely cleared the bacteria from lung tissue after 48 hours, whereas a dose of 8 x $10^8$ –
208 2 x $10^9$ was lethal to all mice within 12 hours. At a dose of 3 x $10^8$, the mice developed
209 symptoms which resolved within 12 hours, and therefore using this dosage we sought to test
210 whether there was a difference in bacterial proliferation and dissemination dependent on the
211 T7SS. However, after 24 hours of infection with 3 x $10^8$ cfu of RN6390 or a cognate Δ*essC*

212 strain, counts recovered from the lungs and livers of mice infected with the Δ*essC* strain were
213 not significantly different than those from mice infected with the wild type (Fig S4).

214 Given that there are likely to be roles for the T7SS in bacterial competition as well as direct
215 interaction with the host, we next developed a model where these two potentially confounding
216 factors could be investigated. The zebrafish (*Danio rerio*), a widely used vertebrate model for
217 development, has recently been adapted to study bacterial infection by human pathogens[39].
218 The hindbrain ventricle offers a sterile compartment that can be used to follow bacterial
219 interactions *in vivo*[40]. We first assessed the utility of this infection model by testing the effect
220 of dose and temperature on survival for *S. aureus* inoculated into the hindbrain ventricle (Fig
221 S5A) of zebrafish larvae 3 days post fertilisation (dpf). Clear dose-dependent zebrafish
222 mortality was observed, with ~90% of zebrafish surviving a low dose of *S. aureus* infection (7
223 x $10^3$ cfu) whereas only ~55% survived a higher dose (2 x $10^4$ cfu; Fig S5B). Although 28.5°C
224 is the optimum temperature for zebrafish larvae development, *S. aureus* has a temperature
225 optimum of 30 - 37°C for growth. In agreement with this, we observed significantly increased
226 zebrafish mortality at 33°C relative to 28.5°C, at high dose infection (Fig S5B).

227 We next assessed whether there was a role for the T7SS in zebrafish mortality. For these
228 experiments, larvae at 3 dpf were inoculated in the hindbrain ventricle with 2 x $10^4$ cfu of
229 RN6390 or an isogenic strain, RN6390 Δ*ess*, lacking all 12 genes (*esxA* through *esaG*) at the
230 *ess* locus[3], and incubated at 33°C. We routinely observed that zebrafish mortality was
231 significantly reduced, at both 24 and 48 hr post inoculation (hpi), for fish infected with the
232 RN6390 Δ*ess* strain compared to the wild type (Fig S5C; Fig 4A,C). In agreement with this,
233 total bacterial counts of infected fish revealed that following an initial period of six hours where
234 both strains replicated in a similar manner, there was a significant decrease in recovery of the
235 Δ*ess* strain compared to the wild type after 9 hours (Fig S5D), suggesting that bacteria lacking
236 the T7SS are more rapidly cleared *in vivo*. We also tested a second *S. aureus* strain, COL, in
237 this assay. Fig S6A shows that COL was only weakly virulent at 24 hpi, but at high dose
238 substantial mortality was seen after 48 hr (Fig S6A). As before, fish mortality was at least in

239 part dependent on a functional T7SS (Fig S6B), although we observed no difference in
240 bacterial burden between the wild type and Δ*essC* strain at the timepoints sampled (FigS6C).
241 We conclude that the T7SS plays a role in virulence of *S. aureus* in this zebrafish infection
242 model.

243 In addition to TspA, a second T7SS secreted toxin, EsaD (also called EssD[9, 41]), has been
244 identified in some *S. aureus* nuclease strains. EsaD was shown to inhibit growth of a
245 competitor *S. aureus* strain *in vitro*[6], but has also been directly implicated in virulence through
246 modulation of cytokine responses and abscess formation[9, 41]. We therefore determined
247 whether TspA or EsaD was required for virulence in the zebrafish infection model. Infection of
248 larvae with strain RN6390 lacking TspA resulted in levels of mortality intermediate between
249 the wild type and Δ*ess s*train (Fig 4A), and a significantly reduced bacterial burden relative to
250 the wild type strain at 9 hpi (Fig 4B). By contrast, no difference was observed in either zebrafish
251 mortality (Fig 4C) or bacterial burden (Fig 4D) between infection with RN6390 and an isogenic
252 *esaD* mutant, indicating no detectable role of EsaD in virulence (Fig 4C, 4D). Taken together,
253 we conclude that zebrafish infection can be used to investigate the role of T7SS effectors *in*
254 *vivo*, and that TspA (but not EsaD) contributes to T7SS-mediated virulence.

255

256 **T7SS dependent bacterial competition *in vivo*.**

257 Although TspA is clearly required for full *S. aureus* virulence in the zebrafish model, the
258 observed toxicity when heterologously produced in *E. coli* coupled with the presence of
259 immunity genes encoded downstream of *tspA* strongly suggests that secreted TspA may also
260 have antibacterial activity. Previously, the antibacterial activity of EsaD was demonstrated
261 using the *S. aureus* COL strain, and required *esaD* to be overproduced from a multi-copy
262 plasmid in order to observe growth inhibition of sensitive *S. aureus* strains[6]. We therefore first
263 tested whether overproduction of TspA in COL could inhibit the growth of strain RN6390 that
264 was deleted for *tspA* along with the 10 genes encoding TsaI homologues. However co-culture

265 experiments in solid or liquid growth conditions failed to demonstrate any TspA-dependent
266 growth inhibition (data not shown).

267 Zebrafish larvae have recently been adapted to study predator-prey interactions[40], and we
268 reasoned that since the T7SS was active in our zebrafish infection model it may also provide
269 a suitable experimental system to investigate the impact of T7-mediated bacterial competition
270 *in vivo*. COL as the attacker strain was co-inoculated into the hindbrain ventricle, at a 1:1 ratio,
271 with either RN6390 or an isogenic strain lacking immunity proteins for EsaD and TspA (FRU1;
272 RN6390 Δ*saouhsc00268-00278*, Δ*saouhsc00585-00602*). A significant reduction in recovery
273 of the target strain lacking immunity genes was observed compared to the isogenic parental
274 strain at 15 hr post infection (Fig 5A). Conversely, there was significantly greater fish mortality
275 at 24 hr after co-inoculation of COL with the wild type RN6390 than the immunity mutant strain
276 (Fig 5B). Since COL is almost completely avirulent at this time-point (Fig S5) we infer that the
277 mortality arises from RN6390, and as the wild type strain survives better when co-inoculated
278 with COL than the immunity deletion strain co-inoculated with COL, this accounts for the
279 greater fish mortality.

280 To confirm that the reduced growth of the RN6390 immunity mutant strain was dependent
281 upon a functional T7SS in the attacking strain, we repeated the co-inoculation experiments
282 using a T7 mutant strain of COL (COLΔ*essC*). The RN6390 immunity mutant strain showed
283 significantly higher recovery after 15 hours in the presence of the COL T7 mutant strain than
284 wild type COL (Fig 5C) and accordingly this was linked with poorer survival of zebrafish (Fig
285 5D). Collectively these data highlight the utility of zebrafish for investigating *S. aureus*
286 competition *in vivo*, and demonstrate that bacterial competition and zebrafish mortality is
287 dependent on a functional T7SS in the attacking strain and the absence of immunity proteins
288 against EsaD and TspA in the prey strain, highlighted in the schematic (Fig 5E).

289 Finally, we investigated which of the EsaD and TspA toxins was responsible for inter-strain
290 competition by using variants of COL deleted for either *tspA* or *esaD* as the attacking strain. It

291 was seen that in the absence of either TspA (Fig 5F) or EsaD (Fig 5H) there was a significant
292 increase in recovery of the RN6390 Δ*saouhsc00268-00278*, Δ*saouhsc00585-00602* prey
293 strain, indicating that each of these toxins has activity against the target strain. However, there
294 was a more pronounced increase in zebrafish mortality when the attacker strain lacked *esaD*
295 than *tspA* (compare Figs 6G and I), suggesting that EsaD has the more potent antibacterial
296 activity in these conditions.

297

298 **Discussion**

299 Here we have taken an unbiased approach to discover substrates of the T7SS in *S. aureus*
300 RN6390, identifying the LXG-domain protein, TspA. TspA localizes to the cell envelope and
301 has a toxic C-terminal domain that has membrane-depolarizing activity. While all other
302 previously-identified T7 substrates are encoded at the *ess* locus and are associated with
303 specific *essC* subtypes[19, 42], TspA is encoded elsewhere on the genome, and is conserved
304 across all *S. aureus* strains. This suggests TspA plays a key role in *S. aureus*, and indeed we
305 show that it contributes to T7SS-mediated virulence in a zebrafish infection model. Pore- and
306 channel-forming toxins are key virulence factors produced by many pathogenic bacteria[43], that
307 can act both extracellularly to form pores in eukaryotic cells, like some bacterial hemolysins[44],
308 or intracellularly for example by altering permeability of the phagosome, like the pore-forming
309 toxin Listeriolysin-O, or the Type III secretion system effector VopQ[45, 46]. It should be noted
310 that the T7SS of strain USA300 has been shown to play a role in release of *S. aureus* during
311 intracellular infection[47], however RN6390 is only poorly invasive in bronchial epithelial cell
312 lines, and intracellular survival and bacterial release is independent of the T7SS (data not
313 shown). The precise mechanism by which TspA interacts with host cells remains to be
314 determined.

315 TspA is a highly unusual toxin because it also has antibacterial activity, leading to growth
316 inhibition of a target *S. aureus* strain *in vivo*. Protection from TspA intoxication is mediated by

317 a genetically-linked immunity protein, TsaI. It is interesting to note that the C-terminal domain
318 of TspA is polymorphic (Fig S7) and that clusters of *tsaI* homologues are encoded at the *tspA*
319 locus, indicative of intraspecies competition with strains accumulating multiple *tsaI*-encoding
320 genes as a likely protective mechanism from TspA sequence variants.

321 In conclusion we have identified an extracellular toxin that can target across the domains of
322 life under the same *in vivo* conditions. To our knowledge it is only the second bacterial exotoxin
323 identified to have such dual-targeting activity, after VasX from *Vibrio cholerae*[48, 49], and the first
324 from Gram positive bacteria.

325 **Materials and Methods**

326 **Bacterial strains, plasmids and growth conditions.** All strains and plasmids used in this
327 study are given in Tables S2 and S3. *S. aureus* strain RN6390[50] and its Δ*essC*[3], Δ*esaD*[6],
328 Δ*SAOUHSC_00268-00278*[6] and Δ*ess* (Δ*esxA-esaG*)[3] derivatives along with strain COL[51]
329 have been described previously. An in-frame deletion of *tspA* (*SAOUHSC_00584*) in RN6390
330 was constructed by allelic exchange using plasmid pIMAY (Table S3)[52]. The upstream and
331 downstream regions including the start codon and last six codons were amplified from RN6390
332 genomic DNA using primers listed in Table S4 and were cloned into pIMAY and introduced
333 onto the chromosome by recombination as described previously[52]. For deletion of *tsaI* and its
334 homologues, the upstream regions of *SAOUHSC_00585* including its first four codons and the
335 downstream *SAOUHSC_00602* including its last four codons were amplified from RN6390
336 genomic DNA, cloned into pIMAY and was introduced into strain RN6390Δ*SAOUHSC_00268-*
337 *00278* to generate strain FRU1 (as RN6390 Δ*SAOUHSC_00268-00278*, Δ*SAOUHSC_00585-*
338 *00602*). For in frame deletion of *esaD* (SACOL0281) and *tspA* (SACOL0643) in strain COL,
339 constructs pIMAY-esaD[6] and pIMAY-tspA were used, following the protocol of[52]. Derivatives
340 of strains harbouring markerless *gfp* or *mCherry* chromosomal insertions were constructed
341 according to[53] using plasmids pTH100 and pRN111, respectively. *E. coli* strain JM110 was
342 used for cloning purposes and MG1655[54] and its isogenic Δ*tatABCD* derivative SG3000[55] was
343 used for toxicity assays.

344 All oligonucleotides used in this study are listed in Table S4, and RN6390 chromosomal DNA
345 was used as template unless otherwise stated. Plasmid pRAB11-tspA-myc encodes TspA with
346 a C-terminal Myc tag in pRAB11[56] and was constructed following amplification with primers
347 tspA cmyc fw and tspA cmyc rv. Plasmid pRAB11-02448-ha produces SAOUHSC_02448 with
348 a C-terminal HA tag from vector pRAB11 and the encoding gene was amplified using primers
349 02448 cha fw and 02448 cha rv. Plasmid pRAB11-0389-ha codes for SAOUHSC_0389 with
350 a C-terminal HA tag in pRAB11 and was constructed following amplification with primers
351 00389 cha fw and 00389 cha rv. Plasmid pRAB11-0406-myc encodes SAOUHSC_0406 with

352 a C-terminal Myc tag in pRAB11 and was constructed following amplification with primers
353 00406 cmyc fw and 00406 cmyc rv. In each case the amplified gene is preceded by the *esxA*
354 RBS (AGGAGGTTTCTAGTT), and were cloned as *Kpn*I - *Sac*I fragments. Plasmid pRMC2-
355 ssaA-ha codes for SsaA with a C-terminal HA tag. It was constructed following amplification
356 of SsaA using primers pRMC2-ssaA-bglII-for and pRMC2- SSaA-HA-rev-EcoRI, digestion with
357 *Bgl*II and *Eco*RI and cloning into similarly cut pRMC2[57].
358 Plasmid pBAD18-tspA codes for the full length TspA. The encoding gene was amplified using
359 primers tspA fl fw and tspA fl rv, digested with *Xba*I and *Sal*I and subsequently cloned into
360 similarly cut pBAD18-Cm[58]. Plasmid pBAD18-tspA$_{CT\ en}$codes for the last 251aa of TspA; the
361 encoding DNA was amplified using primers tspA cp fw and tspA fl rv, digested with *Xba*I and
362 *Sal*I and cloned into similarly cut pBAD18-Cm. Plasmid pBAD18-AmiAss-tspA$_{CT}$ codes for the
363 *E. coli* AmiA signal sequence fused in-frame to the N-terminus of TspA$_{CT}$. This was
364 constructed following separate amplification of the DNA encoding the first 36 amino acids of
365 AmiA using primers AmiAss fw and AmiAss rv with *E. coli* MG1655 chromosomal DNA as
366 template digestion with *Nhe*I and *Kpn*I and cloning into similarly cut pBAD18-Cm. The TspA$_{CT}$
367 coding sequence was then amplified using tspA cp fw (which lacks a start codon) and tspA fl
368 rv, digested with *Xba*I and *Sal*I and cloned into similarly cut pBAD18-AmiAss. Plasmid
369 pBAD18-AmiAss-tspA$_{CT}$ + tsaI codes for the AmiAss-TspA$_{CT}$ fusion along with TsaI. The *tsaI*
370 (*saouhsc_00585*) gene was amplified using primers tsaI fw and tsaI rv, digested with *Sal*I and
371 *Sph*I and cloned into similarly cut pBAD18-AmiAss-tspA$_{CT}$.
372 Plasmid pSUPROM-TsaI produces TsaI constitutively from the *E. coli tat* promoter. The
373 encoding gene was amplified using primers pSU-TsaI fw and pSU-TsaI rv, digested with
374 *Bam*HI and *Xho*I and cloned into similarly-digested pSUPROM[59].
375 *S. aureus* strains were cultured in RPMI medium for proteomic analysis, as detailed below.
376 For all other experiments *S. aureus* strains were grown in TSB medium at 37°C with vigorous
377 agitation. Chloramphenicol was used 10 µg/ml final concentration for plasmid selection.
378 Anhydrotetracycline (ATC) was added to *S. aureus* cultures at 1 µg/ml during allelic gene
379 replacement. For induction of plasmid-encoded proteins, 500 ng/ml ATC was added to

380 cultures at $OD_{600}$ of 0.4, and cells were harvested at $OD_{600}$ of 2.0. *E. coli* was grown aerobically
381 in LB at 37°C, supplemented with ampicillin (100 µg/ml), kanamycin (50 µg/ml) or
382 chloramphenicol (25 µg/ml) where appropriate. D-glucose and L-arabinose were used to
383 control expression of cloned genes from the pBAD18-Cm vector[58]. For toxicity assays single
384 colonies of MG1655 freshly transformed with the appropriate pBAD18-Cm construct growing
385 on LB agar containing 0.2% D-glucose were picked and re-suspended in LB to an $OD_{600}$ of
386 1.0. Serial dilutions to $10^{-5}$ were prepared and 5 µL of each spotted onto LB agar supplemented
387 with 0.2% D-glucose, 0.02% L-arabinose or 0.2% L-arabinose and incubated overnight at
388 37°C.
389
390 **Preparation of culture supernatants for proteomic analysis.** *S. aureus* strains were grown
391 overnight in 2 mL TSB after which cells were harvested, washed three times with 10 mL of
392 RPMI medium, resuspended in 2 mL of RPMI and used to inoculate 200 mL RPMI in 2 L
393 baffled flasks. Cultures were grown at 37°C with vigorous agitation until an $OD_{600}$ of 1.0 was
394 reached, after which cultures were cooled to 4°C, cells pelleted and supernatant proteins
395 precipitated with 6% trichloroacetic acid (TCA) on ice overnight. The precipitated protein
396 samples were harvested by centrifugation (15 min at 18000 *g*) re-suspended in 80% acetone
397 (-20°C) and washed twice with 80% acetone. Pellets were air dried at room temperature and
398 transferred to the mass-spectrometry facility for proteomic analysis.
399
400 **Mass spectrometry data analysis and label-free quantitation.** Sample preparation and
401 mass spectrometry analysis was performed similar to previously described work[60-63].
402 Precipitated proteins were re-dissolved in 1% sodium 3-[(2-methyl-2-undecyl-1,3-dioxolan-4-
403 yl)methoxy]-1-propanesulfonate (commercially available as RapiGest, Waters), 50 mM Tris-
404 HCl pH 8.0, 1 mM TCEP. Cysteines were alkylated by addition of 20 mM Iodoacetamide and
405 incubation for 20 min at 25°C in the dark and the reaction quenched by addition of 20 mM
406 DTT. Samples were diluted to 0.1% Rapigest with 50 mM Tris-HCl pH 8.0 and Trypsin

407 (sequencing grade, Promega) was added at a 1:50 ratio. Proteins were digested overnight at
408 37°C under constant shaking.
409 Samples from four biological replicates (0.5 µg of digest for the secretome analyses) were
410 injected in an interleaved manner onto a 2 cm x 100 µm trap column and separated on a 50
411 cm x 75 µm EasySpray Pepmap C18 reversed-phase column (Thermo Fisher Scientific) on a
412 Dionex 3000 Ultimate RSLC. Peptides were eluted by a linear 3-hour gradient of 95% A/5% B
413 to 35% B (A: $H_2O$, 0.1% Formic acid (FA); B: 80% ACN, 0.08% FA) at 300 nl/min into a LTQ
414 Orbitrap Velos (Thermo-Fisher Scientific). Data was acquired using a data-dependent "top 20"
415 method, dynamically choosing the most abundant precursor ions from the survey scan (400-
416 1600 Th, 60,000 resolution, AGC target value $10^6$). Precursors above the threshold of 2000
417 counts were isolated within a 2 Th window and fragmented by CID in the LTQ Velos using
418 normalised collision energy of 35 and an activation time of 10 ms. Dynamic exclusion was
419 defined by a list size of 500 features and exclusion duration of 60 s. Lock mass was used and
420 set to 445.120025 for ions of polydimethylcyclosiloxane (PCM).
421 Label-free quantitation was performed using MaxQuant 1.5.7.4[64]. Data were searched against
422 the Uniprot database of *S. aureus* NCTC8325 (downloaded on 29.03.17) containing 2,889
423 sequences and a list of common contaminants in proteomics experiments using the following
424 settings: enzyme Trypsin/P, allowing for 2 missed cleavage, fixed modifications were
425 carbamidomethyl (C), variable modifications were set to Acetyl (Protein N-term), Deamidation
426 (NQ) and Oxidation (M). MS/MS tolerance was set to 0.5 Da, precursor tolerance was set to
427 6 ppm. Peptide and Protein FDR was set to 0.01, minimal peptide length was 7, and one
428 unique peptide was required. Re-quantify and retention time alignment (2 min) were enabled.
429 If no intensities were detected in one condition and the other condition had intensities in at
430 least in 3 out of 4 replicates, values were imputed in Perseus v1.5.1.1 using default
431 parameters[65]. A student's t-test (two-tailed, homoscedastic) was performed on the LFQ
432 intensities and only proteins with $p<0.05$ and a fold-change >2-fold were considered
433 significant.
434

435 **Data availability statement.** Raw mass spectrometry data that support the findings of this
436 study have been deposited to the ProteomeXchange Consortium via the PRIDE[66] partner
437 repository with the dataset identifier PXD00XXXX. All other data supporting the findings of this
438 study are available within the paper and its supplementary information files.
439
440 **Cell fractionation and western blotting.** Preparation of *S. aureus* cell and supernatant
441 samples for western blotting, and subcellular fractionation of *S. aureus* into cell wall,
442 membrane and cytoplasmic fractions were as described previously[3]. Preparation of urea-
443 washed membrane fractions was adapted from[67]. Briefly, broken cell suspensions were
444 thoroughly mixed with a final concentration of 4M urea and incubated for 20 minutes at room
445 temperature. Membranes were harvested by ultracentrifugation (227 000 x *g*, 30 min). The
446 supernatant was retained as the urea-treated cytoplasmic fraction and the membrane pellet
447 resuspended in 1 x PBS, 0.5 % Triton X-100. For spheroplast preparation, the method of [68]
448 was adapted. Briefly, strains were cultured as described above, cells were harvested at $OD_{600}$
449 of 2.0 and resuspended in Buffer A (0.7M sucrose, 20mM maleate, 20mM $MgCl_2$, pH 6.5).
450 Lysostaphin and lysozyme were added at 20 µg/ml and 20 mg/ml final concentration,
451 respectively, and cells incubated at 37°C for 1 hour. Cell debris was pelleted by centrifugation
452 (2,500 x *g* for 8 min) and the resulting supernatant centrifuged at 16,000 x *g* for 10 min to
453 pellet the spheroplasts. Sphaeroplasts wer resuspended in 150 µl of Buffer A and were treated
454 with increasing concentrations of Proteinase K on ice for 30 mins. 50 µM phenylmethylsulfonyl
455 fluoride was added to terminate the reaction and samples mixed with 4x Nu PAGE LDS
456 sample buffer and boiled for 10 min prior to further analysis. Western blotting was performed
457 according to standard protocols using the following antibody dilutions α-EsxA [3] 1:2500; α-
458 EsxC[3] 1:2000, α-EssB[3] 1:10000, α-TrxA[69] 1:25000, α-SrtA (Abcam, catalogue number
459 ab13959) 1:3000, α-HA (HRP-conjugate, Sigma catalogue number H6533) α-Myc (HRP-
460 conjugate, Invitrogen catalogue number R951-25) 1:5000, and goat anti Rabbit IgG HRP
461 conjugate (Bio-Rad, catalogue number 170-6515) 1:10000.
462

463 **Bacterial membrane potential detection.** To assess bacterial membrane potential, the
464 method of [70] was adapted, using the BacLight bacterial membrane potential kit (Invitrogen). In
465 brief, overnight cultures of *E. coli* MG1655 harbouring pBAD18-Cm derivatives were sub-
466 cultured into LB medium containing appropriate antibiotics to an $OD_{600}$ of 0.1 and cultured
467 aerobically to $OD_{600}$ of 0.5, before supplementation with 0.2% L-arabinose. Cells were cultured
468 for a further hour then diluted to 1 x $10^6$ cells per ml in sterile PBS, and a 1ml aliquot of bacterial
469 suspension was added to each flow cytometry tube. For the depolarized control, 25 µL of 500
470 µM carbonyl cyanide m-chlorophenyl hydrazone (CCCP), provided in the BacLight bacterial
471 membrane potential kit, was added. Next, 3 µL of 3mM $DiOC_2(3)$ was added to each sample,
472 which was mixed and incubated at room temperature for 30 minutes. Cells were subsequently
473 sorted using an LSRFortessa cell analyser (BD Biosciences, San Jose, CA). The $DiOC_2(3)$
474 dye was excited at 488 nm, with fluorescent emissions detected at 530 and 685 nm. In total,
475 20000 events were collected for each sample, with forward- and side-scatter parameters used
476 to gate the bacteria. The forward scatter, side scatter, and fluorescence were collected with
477 logarithmic signal amplification. The gated populations were then analysed with FlowJo
478 software by generating a dot plot of red versus green fluorescence.
479 To assess changes in membrane potential and permeabilisation, the same *E. coli* strains were
480 grown as described above. An 'uninduced' sample of *E. coli* harbouring each of pBAD18-Cm
481 (empty), pAmiAss-$TspA_{CT}$ and pAmiAss-$TspA_{CT}$-TsaI was collected and adjusted to $OD_{600}$ of
482 0.2 before the addition of 2 µM $DiSC_3(5)$ and 200 nM Sytox Green. A permeabilised control
483 sample of cells harbouring empty vector and containing 10 µg/ml Polymyxin B was also
484 prepared and supplemented with both dyes. All samples were then incubated at 37°C for 5
485 minutes before being analysed by microscopy. To induce protein production from the pBAD18-
486 Cm vector, cell suspensions were adjusted to $OD_{600}$ of 0.2 and supplemented with 0.2% L-
487 arabinose for the indicated period of time (10-60 min) before incubating with $DiSC_3(5)$ and
488 Sytox Green, as above. Imaging of $DiSC_3(5)$ and Sytox Green stained cells was carried out
489 Nikon Eclipse Ti equipped with Sutter Instrument Lambda LS light source, Nikon Plan Apo
490 100×/1.40 NA Oil Ph3 objective, and Photometrics Prime sCMOS, and Cy5 and GFP filters,

491 respectively. The images were captured using Metamorph 7.7 (Molecular Devices) and
492 analysed using ImageJ. For the analysis, the phase contrast images acquired in parallel to the
493 fluorescence images were used to identify cells as regions of interest, for which average
494 $DiSC_3(5)$ and Sytox Green fluorescence intensity was measured from the corresponding
495 background-subtracted fluorescence images. Data was then plotted as a scatter plot for
496 $DiSC_3(5)$ and Sytox Green fluorescence with each point representing an individual cell.
497

498 **Mouse pneumonia model.** *S. aureus* RN6390 (WT) or the isogenic Δ*essC* strain were
499 subcultured at 1:100 dilution from an overnight culture into fresh TSB medium. Cells were
500 grown at 37°C with shaking until an $OD_{600}$ of 0.5 was reached, before harvesting and washing
501 three times in 1x PBS. Cells were finally resuspended in 1 x PBS to 1.2 x $10^{10}$ cfu/ml. Female
502 10-12 week old C57/B6 J mice were purchased from Charles River U.K.. Mice were
503 acclimatised for a 10 day period prior to starting the experiment. Mice were randomised to
504 cages and treatment groups, and analyses were performed blind. Mice were anaesthetized
505 (gaseous isofluorane) and infected intranasally with 25 µL of the bacterial suspension to give
506 a final infected dose of 3 x $10^8$ cfu per mouse. At 24 hours post infection the lungs and livers
507 were harvested and the bacterial load determined by plating serial dilutions of tissue
508 homogenates.
509

510 **Zebrafish Infection.** Wild-type (WT, AB strain) or transgenic Tg(*lyz*::dsRed)$^{nz50}$ [71] zebrafish
511 were used for all experiments. Embryos were obtained from naturally spawning zebrafish, and
512 maintained at 28.5°C until 3 days post fertilisation (dpf) in embryo medium (0.5x E2 medium
513 supplemented with 0.3 g/ml methylene blue)[72]. For injections, larvae were anesthetized with
514 200 µg/ml tricaine (Sigma-Aldrich) in embryo medium. Hindbrain ventricle infections were
515 carried out at 3 dpf and incubated at 33°C unless specified otherwise. Bacteria were
516 subcultured following overnight growth until they reached $OD_{600}$ of 0.6. For injection of larvae,
517 bacteria were recovered by centrifugation, washed and resuspended in 1x PBS, 0.1% phenol

518 red, 1% polyvinylpyrrolidone to the required cfu/ml. Anaesthetized larvae were microinjected
519 in the hindbrain ventricle (HBV) with 1–2 nL of bacterial suspension. At the indicated times,
520 larvae were sacrificed in tricaine, lysed with 200 µL of 0.4% Triton X-100 and homogenized
521 mechanically. Larval homogenates were serially diluted and plated onto TSB agar. Only larvae
522 having survived the infection were included for enumeration of colony-forming units (cfu). For
523 zebrafish virulence assays all *S. aureus* strains were chromosomally tagged with GFP which
524 included RN6390 wild type, and isogenic Δ*ess*, Δ*tspA* and Δ*esaD* strains. For *in vivo*
525 competition experiments, COL (attacker) strains were chromosomally-tagged with mCherry
526 and RN6390 (target) strains with GFP. Attacker and target strains were subcultured, harvested
527 and resuspended in PBS as above. Attacker and target strains were mixed at a 1:1 ratio and
528 injected in the hindbrain ventricle, with 1-2 nL of bacterial suspension. Larvae were sacrificed
529 at 15 hpi or 24 hpi, serially diluted and plated on TSB agar, and attacker and target strains
530 were enumerated by fluorescence (GFP and mCherry).

531 **Acknowledgements**

532 This study was supported the Wellcome Trust [through Early Postdoctoral Training Fellowship
533 for Clinician Scientists WT099084MA to JDC, Investigator Award 110183/Z/15/Z to TP and
534 Institutional Strategic Support Fund 105606/Z/14/Z to the University of Dundee], the UK
535 Biotechnology and Biological Sciences Research Council [grants BB/H007571/1 and
536 EASTBIO DTP1 grant ref BB/J01446X/1], The Microbiology Society (through a Research Visit
537 Grant awarded to FRU) and a China Scholarship Council PhD studentship (to ZC). MT was
538 funded by the Medical Research Council UK through grant MC_UU_12016/5. Work in the SM
539 laboratory is supported by a Wellcome Trust Senior Research Fellowship (206444/Z/17/Z),
540 Wellcome Trust Research Career Development Fellowship (WT097411MA) and the Lister
541 Institute of Preventive Medicine. We thank Professor Frank Sargent and Dr Sabine Grahl for
542 providing us with *E. coli* strain SG3000, Professor Jan-Maarten van Dijl (University of
543 Groningen) for the kind gift of anti-TrxA antiserum, and Drs Giuseppina Mariano, Sarah
544 Coulthurst, Vincenzo Torraca, Margarida Gomes and Melanie Blokesch for helpful discussion
545 and advice.

546 **Figure legends**

547 **Figure 1. The *S. aureus* RN6390 T7 secretome.** A. the *ess* locus in strain NCTC8325 (parent
548 of RN6390). Genes for core components are shaded green, secreted substrates yellow, EsaE
549 (which is co-secreted with EsaD) in hatched shading and the cytoplasmic antitoxin EsaG in
550 white. B. Growth of RN6390 (WT) and the isogenic Δ*essC* strain in RPMI medium. C. RN6390
551 (WT) and the Δ*essC* strain cultured in RPMI growth medium to $OD_{600}$ = 1. Samples were
552 separated into supernatant (sn) and cellular (c) fractions (12% bis-Tris gels) and
553 immunoblotted with anti-EsxA, anti-EssB, anti-EssC or anti-TrxA (cytoplasmic protein)
554 antisera. D. Volcano plot of the quantitative proteomic secretome analysis. Each spot
555 represents an individual protein ranked according to its statistical p-value (y-axis) and relative
556 abundance ratio (log2 fold change). The blue dotted lines represent cut-offs for significance
557 ($p<0.05$; log2 fold-change>1). E. Proteins present in the secretome of RN6390 at an
558 abundance of greater than 2-fold higher than the secretome of the isogenic ΔessC strain. A
559 full list of all of the proteins identified in this analysis is given in Table S1. *not detected in the
560 Δ*essC* secretome.

561 **Figure 2. SAOUHSC_00584/TspA is an extracellular peripheral membrane protein.** A.
562 RN6390 (WT) and the Δ*essC* strain harbouring pRAB11 (empty) or pRAB11-TspA-Myc were
563 cultured in TSB growth medium. Following induction of plasmid-encoded TspA-Myc
564 production, cells were harvested and fractionated into cell wall (cw), membrane (m) and
565 cytoplasmic (cyt) fractions. Samples were separated (12% bis-Tris gels) and immunoblotted
566 with anti-Myc-HRP anti-TrxA (cytoplasmic protein), anti-Spa (cell wall) or anti-SrtA
567 (membrane) antisera. * 'non-specific' cross-reacting band corresponding to Spa. B. Cell
568 extracts from the RN6390 samples in (A) were incubated with 4M urea, membranes were
569 isolated and the urea-treated cytoplasm (cyt+) and membranes (m+) were separated
570 alongside the cell wall and untreated cytoplasm and membrane fractions on a 12% bis-tris gel
571 and immunoblotted with anti-Myc and anti-SrtA antisera. C. Spheroplasts from strain RN6390

572 producing TspA-Myc were incubated with the indicated concentrations of Proteinase K (pk) at
573 4°C for 30 mins. A sample of spheroplasts from RN6390 containing pRAB11 (empty) is shown
574 as a negative control. Samples were separated on a 12% bis-tris gel and immunoblotted using
575 anti-Myc, anti-SrtA, anti-EssB and anti-TrxA antisera. D. *S. aureus* RN6390 or the isogenic
576 Δ*essC* or Δ*tspA* strains were cultured in TSB medium and harvested at $OD_{600}$ of 2.
577 Supernatant (sn) and cellular (c) fractions (equivalent of 100 µL culture supernatant and 10
578 µL of cells adjusted to $OD_{600}$ of 2.0) were separated on bis-Tris gels (15% acrylamide) and
579 immunoblotted using anti-EsxA, EsxC or TrxA antisera. E. Model for organization of TspA in
580 the *S. aureus* envelope. CTD – C-terminal (channel-forming) domain.

581 **Figure 3. Directed export of TspA C-terminal domain to the periplasm of *E. coli* is toxic**
582 **and disrupts the membrane potential**. A. Structural model for residues 9-416 of TspA
583 generated using RaptorX (http://raptorx.uchicago.edu/), modelled on the colicin Ia structure [27].
584 The predicted channel-forming region is shown in yellow. B. The *tspA* locus. Genes coding for
585 DUF443 proteins are shown in yellow. C. *E. coli* strain MG1655 harbouring empty pBAD18-
586 Cm or pBAD18-Cm encoding either full length TspA, the TspA C-terminal domain ($TspA_{CT}$),
587 $TspA_{CT}$ with the AmiA signal sequence at its N-terminus (AmiAss-$TspA_{CT}$), AmiAss-$TspA_{CT}$
588 and TsaI (SAOUHSC_00585), AmiAss-$TspA_{CT}$/TsaI alongside an additional plasmid-encoded
589 copy of TsaI (from Psu-TsaI) or strain SG3000 (as MG1655, Δ*tatABCD*) harbouring pBAD18-
590 AmiAss-$TspA_{CT}$ was serially diluted and spotted on LB plates containing either D-glucose or
591 L-arabinose, as indicated. Plates were incubated at 37°C for 16 hours after which they were
592 photographed. D. *E. coli* MG1655 harbouring pBAD18-Cm (empty), or pBAD18-Cm encoding
593 AmiAss-$TspA_{CT}$ or AmiAss-$TspA_{CT}$ / TsaI were grown in the presence of 0.2% L-arabinose for
594 1 hour at which point they diluted to 1 x $10^6$ cells per ml and supplemented with 30 µM
595 $DiOC_2(3)$ for 30 mins. One sample of MG1655 harbouring pBAD18 (empty) was also
596 supplemented with 5 µM CCCP at the same time as $DiOC_2(3)$ addition. Strains were analyzed
597 by flow cytometry. E-G. The same strain and plasmid combinations as D were grown in the
598 presence (induced) or absence (uninduced) of 0.2% L-arabinose for 30 minutes after which

599 they were supplemented with $DiSC_s(5)$ and Sytox Green and E. imaged by phase contrast
600 and fluorescence microscopy. F+G. Fluorescence intensities of F. $DiSC_3(5)$ and G. Sytox
601 Green for each sample was quantified using image J. A control sample where Polymyxin B
602 was added to the uninduced empty vector control for 5 minutes before supplemented with
603 $DiSC_s(5)$ and Sytox Green was included in each experiment.

604 **Figure 4. The T7SS contributes to virulence in a zebrafish infection model.** A. Survival
605 curves of 3 dpf zebrafish lyz:dsRed larvae infected in the hindbrain ventricle with RN6390-gfp
606 (WT) or otherwise isogenic Δ*ess*-gfp or Δ*tspA*-gfp strains at a dose of ~2 x $10^4$ cfu and
607 incubated at 33°C for 48 hpi. Data are pooled from five independent experiments (*n*=17-51
608 larvae per experiment). The p value between conditions was determined by log-rank Mantel-
609 Cox test. B. Enumeration of recovered bacteria at 0, 6, 9 or 24 hpi from zebrafish larvae
610 infected with the same strains as A. Pooled data from 3 independent experiments. Circles
611 represent individual larva, and only larvae that survived the infection were included. No
612 significant differences observed between strains at 0, 6 or 24 hpi. Mean ± SEM also shown
613 (horizontal bars). Significance testing performed by unpaired *t* test. C. Survival curves of 3 dpf
614 zebrafish lyz:dsRed larvae infected in the hindbrain ventricle with RN6390-gfp (WT) or
615 otherwise isogenic Δ*ess*-gfp, Δ*esaD*-gfp strains at a dose of ~2 x $10^4$ cfu and incubated at
616 33°C for 48 hpi. Data are pooled from three independent experiments (*n*=26-32 larvae per
617 experiment). Results are plotted as a Kaplan-Meier survival curve and the p value between
618 conditions was determined by log-rank Mantel-Cox test. D. Enumeration of recovered bacteria
619 at 0, 6, 9 or 24 hpi from zebrafish embryos infected with the strains as C. Pooled data from 3
620 independent experiments. Circles represent individual larva, and only larvae having survived
621 the infection were included. No significant differences observed between strains at 0, 6 or 24
622 hpi. Mean ± SEM also shown (horizontal bars). Significance testing performed by unpaired *t*
623 test. **p<0.01, *** p<0.001, **** p<0.0001, ns, not significant.

624 **Figure 5. Development of an *in vivo* model to study bacterial competition**. Wild type AB
625 zebrafish larvae at 3 dpf were co-infected with a 1:1 mix of an attacker strain (either COL-

626 mCherry (WT), COL Δ*essC*-mCherry, COL Δ*tspA*-mCherry or COL Δ*esaD*-mCherry as
627 indicated) and a target strain (either RN6390-gfp (WT) or RN6390 Δ*00268-278* Δ*00585-*
628 *00602*-gfp, as indicated). A, C, F, H. Enumeration of recovered attacker and prey bacteria
629 from zebrafish larvae at 0, 15 or 24 hpi. Pooled data from 3 independent experiments, Mean
630 ± SEM also shown (horizontal bars). Significance testing performed by unpaired *t* test. B, D,
631 G, I. Survival curves of zebrafish injected with the indicated strain pairs. Data are pooled from
632 three independent experiments. Results are plotted as a Kaplan-Meier survival curve and the
633 p value between conditions was determined by log-rank Mantel-Cox test. **p<0.01, ***
634 p<0.001, **** p<0.0001, ns, not significant. E. Model highlighting the role for the T7SS in
635 competition *in vivo*.

636 **Figure S1. HA-tagged variants of SAOUHSC_00389, SAOUHSC_02448 and SsaA are not**
637 **secreted by the T7SS.** The wild type RN6390 and Δ*essC* mutant carrying A-D pRAB11
638 (empty) or pRAB11 encoding A. C-terminally HA-tagged SAOUHSC_00389; B. C-terminally
639 Myc-tagged SAOUHSC_00406; C. C-terminally Myc-tagged tagged SAOUHSC_00584; D. C-
640 terminally HA-tagged SAOUHSC_02448, or E. pRMC2 (empty) or encoding C-terminally HA-
641 tagged SsaA were cultured in TSB medium and supplemented with 200 ng/ml ATc at $OD_{600}$ of
642 0.5. Wen cultures reached $OD_{600}$ of 3.0, samples were withdrawn and separated into culture
643 supernatant (sn) and cellular (c) fractions. Samples were separated on 12% bis-Tris gels and
644 immunoblotted with anti-HA, anti-Myc, anti-EsxA or anti-TrxA antibodies, as indicated.

645 **Figure S2. Peptide coverage of TspA from proteomic analysis.** Regions of TspA coloured
646 orange were detected by mass spectroscopy analysis.

647 **Figure S3. Rapid membrane depolarization by the C-terminal domain of TspA.**
648 Fluorescence intensity changes in $DiSC_3(5)$ (left) and Sytox Green (right) in uninduced cells
649 harbouring pBAD18-Cm (empty), pBAD18-AmiAss-$TspA_{CT}$ and pBAD18-AmiAss-$TspA_{CT}$ and
650 upon induction with 0.2% L-arabinose. Cells were then induced for 10, 30 and 60 minutes
651 before samples removed and cells incubated with $DiSC_3(5)$ and Sytox Green. Fluorescence

652 intensity of $DiSC_3(5)$ and Sytox Green also measured upon addition of Polymixin B to empty
653 vector as a control for membrane depolarization and permeabilisation.

654 **Figure S4. No difference in bacterial burden between wild type and *essC* mutant strains**
655 **in a 24 hour murine pneumonia infection model.** Female 10-12 week old C57/B6 mice
656 were challenged with 3 x $10^8$ cfu/ml of RN6390 (WT) or the isogenic Δ*essC* strain. Bacterial
657 load was determined in liver and lungs 24 hours after infection. Mean ± SEM (horizontal bars)
658 is shown. Significance testing performed by unpaired *t* test.

659 **Figure S5. Developing a zebrafish model to assess T7SS activity *in vivo*.** A. Schematic
660 of zebrafish larvae showing the site of *S. aureus* injection into the hindbrain ventricle. B.
661 Survival curves of lyz:dsRed zebrafish larvae injected with wild type RN6390 chromosomally
662 tagged with GFP. Zebrafish were injected at 3 dpf with a low (~7 x $10^3$ cfu), medium (~1.4 x
663 $10^4$ cfu) or high (~2 x $10^4$ cfu) dose of RN6390-gfp, incubated at 28.5°C or 33°C and monitored
664 for 48 hpi. Data are pooled from two independent experiments (*n*=22-25 larvae per
665 experiment). Results are plotted as a Kaplan- Meier survival curve and the *p* value between
666 conditions was determined by log-rank Mantel-Cox test. C. Survival curves of lyz:dsRed larvae
667 infected in the hindbrain 3 dpf with RN6390-gfp or RN6390 Δ*ess*-gfp at a dose of ~2 x $10^4$ cfu
668 and incubated at 33°C for 48 hpi. Data are pooled from three independent experiments (*n*=28-
669 50 larvae per experiment. Results are plotted as a Kaplan-Meier survival curve and the p value
670 between conditions was determined by log-rank Mantel-Cox test. C. Enumeration of recovered
671 bacteria at 0, 3, 6, 9, 24 or 48 hpi from zebrafish embryos infected with RN6390-gfp or RN6390
672 Δ*ess*-gfp. Pooled data from 3 independent experiments. Circles represent individual larva, and
673 only larvae having survived the infection were included. Mean ± SEM also shown (horizontal
674 bars). Significance testing performed using an unpaired *t* test. *p<0.05 **p<0.01, *** p<0.001,
675 **** p<0.0001, ns, not significant.

676 **Figure S6. *S. aureus* COL also exhibits dose and T7SS-dependent zebrafish mortality.**
677 A. Survival curves of WT zebrafish larvae injected with wild type COL chromosomally tagged

678 with mCherry. Zebrafish were injected at 3 dpf with a low (~7 x $10^3$ cfu), medium (~1.5 x $10^4$
679 cfu) or high dose (~2 x $10^4$ cfu) of COL-mCherry, incubated at 33°C and monitored for 48 hpi.
680 Data are pooled from three independent experiments. Results are plotted as a Kaplan-Meier
681 survival curve and the p value between conditions was determined by log-rank Mantel-Cox
682 test. B. Survival curves of zebrafish larvae injected in the hindbrain 3 dpf with COL-mCherry
683 (WT) or COL Δ*essC*-mCherry at a dose of ~1.6 x $10^5$ cfu and incubated at 33°C for 48 hpi.
684 Data are pooled from three independent experiments (*n*=23-30 larvae per experiment).
685 Results are plotted as Kaplan-Meier survival curves and the p value between conditions was
686 determined by the log-rank Mantel Cox test. C. Enumeration of recovered bacteria at 0, 6, 24
687 or 48 hpi from zebrafish embryos infected with COL-mCherry (WT) or COL Δ*essC*-mCherry.
688 Circles represent individual larvae and data pooled data from 3 independent experiments.
689 Mean ± SEM also shown (horizontal bars). *p<0.05 **p<0.01, *** p<0.001, **** p<0.0001, ns,
690 not significant.

691 **Figure S7. TspA proteins encoded by *S. aureus* strains show variability within the**
692 **channel-forming domain.** A selection of TspA protein sequences encoded by *S. aureus*
693 strains were extracted from NCBI (ncbi.nlm.nih.gov/), aligned using ClustalW
694 (http://www.ch.embnet.org/software/ClustalW.html) and shaded with Boxshade
695 (http://www.ch.embnet.org/software/BOX_form.html

696 **References**


697 1. Groschel, M.I., Sayes, F., Simeone, R., Majlessi, L. & Brosch, R. ESX secretion
698 systems: mycobacterial evolution to counter host immunity. *Nat Rev Microbiol* **14**, 677-
699 691 (2016).
700
701 2. Burts, M.L., Williams, W.A., DeBord, K. & Missiakas, D.M. EsxA and EsxB are secreted
702 by an ESAT-6-like system that is required for the pathogenesis of *Staphylococcus*
703 *aureus* infections. *Proc Natl Acad Sci USA* **102**, 1169-1174 (2005).
704
705 3. Kneuper, H. *et al.* Heterogeneity in ess transcriptional organization and variable
706 contribution of the Ess/Type VII protein secretion system to virulence across closely
707 related *Staphylocccus aureus* strains. *Mol Microbiol* **93**, 928-943 (2014).
708
709 4. Wang, Y. *et al.* Role of the ESAT-6 secretion system in virulence of the emerging
710 community-associated *Staphylococcus aureus* lineage ST398. *Sci Rep* **6**, 25163
711 (2016).
712
713 5. Windmuller, N. *et al.* Transcriptional adaptations during long-term persistence of
714 *Staphylococcus aureus* in the airways of a cystic fibrosis patient. *Int J Med Microbiol*
715 **305**, 38-46 (2015).
716
717 6. Cao, Z., Casabona, M.G., Kneuper, H., Chalmers, J.D. & Palmer, T. The type VII
718 secretion system of *Staphylococcus aureus* secretes a nuclease toxin that targets
719 competitor bacteria. *Nat Microbiol* **2**, 16183 (2016).
720
721 7. Whitney, J.C. *et al.* A broadly distributed toxin family mediates contact-dependent
722 antagonism between gram-positive bacteria. *eLife* **6** (2017).
723
724 8. Klein, T.A., Pazos, M., Surette, M.G., Vollmer, W. & Whitney, J.C. Molecular Basis for
725 Immunity Protein Recognition of a Type VII Secretion System Exported Antibacterial
726 Toxin. *J Mol Biol* pii: S0022-2836(18)30594-1. doi: 10.1016/j.jmb.2018.08.027 (2018).
727
728 9. Ohr, R.J., Anderson, M., Shi, M., Schneewind, O. & Missiakas, D. EssD, a Nuclease
729 Effector of the *Staphylococcus aureus* ESS Pathway. *J Bacteriol* **199** e00528 (2017).
730
731 10. Rosenberg, O.S. *et al.* Substrates Control Multimerization and Activation of the Multi-
732 Domain ATPase Motor of Type VII Secretion. *Cell* **161**, 501-512 (2015).
733
734 11. Zoltner, M. *et al.* EssC: domain structures inform on the elusive translocation channel
735 in the Type VII secretion system. *Biochem J* **473**, 1941-1952 (2016).
736
737 12. Ramsdell, T.L., Huppert, L.A., Sysoeva, T.A., Fortune, S.M. & Burton, B.M. Linked
738 domain architectures allow for specialization of function in the FtsK/SpoIIIE ATPases
739 of ESX secretion systems. *J Mol Biol* **427**, 1119-1132 (2015).
740
741 13. Beckham, K.S. *et al.* Structure of the mycobacterial ESX-5 type VII secretion system
742 membrane complex by single-particle analysis. *Nat Microbiol* **2**, 17047 (2017).
743
744 14. Houben, E.N. *et al.* Composition of the type VII secretion system membrane complex.
745 *Mol Microbiol* **86**, 472-484 (2012).
746
747 15. Mielich-Suss, B. *et al.* Flotillin scaffold activity contributes to type VII secretion system
748 assembly in *Staphylococcus aureus*. *PLoS Pathog* **13**, e1006728 (2017).
749

16. Champion, P.A., Stanley, S.A., Champion, M.M., Brown, E.J. & Cox, J.S. C-terminal signal sequence promotes virulence factor secretion in *Mycobacterium tuberculosis*. *Science* **313**, 1632-1636 (2006).

17. Burts, M.L., DeDent, A.C. & Missiakas, D.M. EsaC substrate for the ESAT-6 secretion pathway and its role in persistent infections of *Staphylococcus aureus*. *Mol Microbiol* **69**, 736-746 (2008).

18. Anderson, M., Aly, K.A., Chen, Y.H. & Missiakas, D. Secretion of atypical protein substrates by the ESAT-6 secretion system of *Staphylococcus aureus*. *Mol Microbiol* **90**, 734-743 (2013).

19. Warne, B. *et al.* The Ess/Type VII secretion system of *Staphylococcus aureus* shows unexpected genetic diversity. *BMC Genomics* **17**, 222 (2016).

20. Anderson, M. *et al.* EssE Promotes *Staphylococcus aureus* ESS-Dependent Protein Secretion To Modify Host Immune Responses during Infection. *J Bacteriol* **199**, e00527 (2017).

21. Dreisbach, A. *et al.* Profiling the surfacome of *Staphylococcus aureus*. *Proteomics* **10**, 3082-3096 (2010).

22. Casabona, M.G. *et al.* Haem-iron plays a key role in the regulation of the Ess/type VII secretion system of *Staphylococcus aureus* RN6390. *Microbiology* **163**, 1839-1850 (2017).

23. Casabona, M.G. *et al.* Functional analysis of the EsaB component of the *Staphylococcus aureus* Type VII secretion system. *Microbiology* **163**, 1851–1863 (2017).

24. Jäger, F., Zoltner, M., Kneuper, H., Hunter, W.N. & Palmer, T. Membrane interactions and self-association of components of the Ess/Type VII secretion system of *Staphylococcus aureus*. *FEBS Letts* **590**, 349-357 (2016).

25. Zoltner, M., Fyfe, P.K., Palmer, T. & Hunter, W.N. Characterization of *Staphylococcus aureus* EssB, an integral membrane component of the Type VII secretion system: atomic resolution crystal structure of the cytoplasmic segment. *Biochem J* **449**, 469-477 (2013).

26. Zoltner, M. *et al.* The Architecture of EssB, an Integral Membrane Component of the Type VII Secretion System. *Structure* **21**, 595-603 (2013).

27. Wiener, M., Freymann, D., Ghosh, P. & Stroud, R.M. Crystal structure of colicin Ia. *Nature* **385**, 461-464 (1997).

28. Kienker, P.K., Qiu, X., Slatin, S.L., Finkelstein, A. & Jakes, K.S. Transmembrane insertion of the colicin Ia hydrophobic hairpin. *J Membr Biol* **157**, 27-37 (1997).

29. Kienker, P.K., Jakes, K.S., Blaustein, R.O., Miller, C. & Finkelstein, A. Sizing the protein translocation pathway of colicin Ia channels. *J Gen Physiol* **122**, 161-176 (2003).

30. Qiu, X.Q., Jakes, K.S., Kienker, P.K., Finkelstein, A. & Slatin, S.L. Major transmembrane movement associated with colicin Ia channel gating. *J Gen Physiol* **107**, 313-328 (1996).

31. Ize, B., Stanley, N.R., Buchanan, G. & Palmer, T. Role of the *Escherichia coli* Tat pathway in outer membrane integrity. *Mol Microbiol* **48**, 1183-1193 (2003).

32. Palmer, T. & Berks, B.C. The twin-arginine translocation (Tat) protein export pathway. *Nat Rev Microbiol* **10**, 483-496 (2012).

33. Seilie, E.S. & Bubeck Wardenburg, J. *Staphylococcus aureus* pore-forming toxins: The interface of pathogen and host complexity. *Seminars in cell & developmental biology* (2017).

34. Jamet, A. & Nassif, X. New players in the toxin field: polymorphic toxin systems in bacteria. *MBio* **6**, e00285-00215 (2015).

35. Kepplinger, B. *et al.* Mode of Action and Heterologous Expression of the Natural Product Antibiotic Vancoresmycin. *ACS Chem Biol* **13**, 207-214 (2018).

36. Daugelavicius, R., Bakiene, E. & Bamford, D.H. Stages of polymyxin B interaction with the *Escherichia coli* cell envelope. *Antimicrob Agents Chemother* **44**, 2969-2978 (2000).

37. Weaver, C.A., Redborg, A.H. & Konisky, J. Plasmid-determined immunity of *Escherichia coli* K-12 to colicin Ia Is mediated by a plasmid-encoded membrane protein. *J Bacteriol* **148**, 817-828 (1981).

38. Bubeck Wardenburg, J., Patel, R.J. & Schneewind, O. Surface proteins and exotoxins are required for the pathogenesis of *Staphylococcus aureus* pneumonia. *Infect Immun* **75**, 1040-1044 (2007).

39. Torraca, V. & Mostowy, S. Zebrafish Infection: From Pathogenesis to Cell Biology. *Trends Cell Biol* **28**, 143-156 (2018).

40. Willis, A.R. *et al.* Injections of Predatory Bacteria Work Alongside Host Immune Cells to Treat *Shigella* Infection in Zebrafish Larvae. *Curr Biol* **26**, 3343-3351 (2016).

41. Anderson, M., Chen, Y.H., Butler, E.K. & Missiakas, D.M. EsaD, a Secretion Factor for the Ess Pathway in *Staphylococcus aureus*. *J Bacteriol* **193**, 1583-1589 (2011).

42. Dai, Y. *et al.* A Novel ESAT-6 Secretion System-Secreted Protein EsxX of Community-Associated *Staphylococcus aureus* Lineage ST398 Contributes to Immune Evasion and Virulence. *Front Microbiol* **8**, 819 (2017).

43. Dal Peraro, M. & van der Goot, F.G. Pore-forming toxins: ancient, but never really out of fashion. *Nat Rev Microbiol* **14**, 77-92 (2016).

44. Gonzalez-Juarbe, N. *et al.* Pore-Forming Toxins Induce Macrophage Necroptosis during Acute Bacterial Pneumonia. *PLoS Pathog* **11**, e1005337 (2015).

45. Hamon, M.A., Ribet, D., Stavru, F. & Cossart, P. Listeriolysin O: the Swiss army knife of Listeria. *Trends Microbiol* **20**, 360-368 (2012).

46. Sreelatha, A. *et al.* Vibrio effector protein, VopQ, forms a lysosomal gated channel that disrupts host ion homeostasis and autophagic flux. *Proc Natl Acad Sci USA* **110**, 11559-11564 (2013).

860 47. Korea, C.G. *et al.* Staphylococcal Esx proteins modulate apoptosis and release of
861 intracellular *Staphylococcus aureus* during infection in epithelial cells. *Infect Immun*
862 **82**, 4144-4153 (2014).
863
864 48. Miyata, S.T., Kitaoka, M., Brooks, T.M., McAuley, S.B. & Pukatzki, S. *Vibrio cholerae*
865 requires the type VI secretion system virulence factor VasX to kill *Dictyostelium*
866 *discoideum*. *Infect Immun* **79**, 2941-2949 (2011).
867
868 49. Dong, T.G., Ho, B.T., Yoder-Himes, D.R. & Mekalanos, J.J. Identification of T6SS-
869 dependent effector and immunity proteins by Tn-seq in *Vibrio cholerae*. *Proc Natl Acad*
870 *Sci USA* **110**, 2623-2628 (2013).
871
872 50. Novick, R.P. *et al.* Synthesis of staphylococcal virulence factors is controlled by a
873 regulatory RNA molecule. *EMBO J* **12**, 3967-3975 (1993).
874
875 51. Dyke, K.G., Jevons, M.P. & Parker, M.T. Penicillinase production and intrinsic
876 resistance to penicillins in *Staphylococcus aureus*. *Lancet* **1**, 835-838 (1966).
877
878 52. Monk, I.R., Shah, I.M., Xu, M., Tan, M.W. & Foster, T.J. Transforming the
879 untransformable: application of direct transformation to manipulate genetically
880 *Staphylococcus aureus* and *Staphylococcus epidermidis*. *MBio* **3** e00277 (2012).
881
882 53. de Jong, N.W., van der Horst, T., van Strijp, J.A. & Nijland, R. Fluorescent reporters
883 for markerless genomic integration in *Staphylococcus aureus*. *Sci Rep* **7**, 43889
884 (2017).
885
886 54. Blattner, F.R. *et al.* The complete genome sequence of *Escherichia coli* K-12. *Science*
887 **277**, 1453-1462 (1997).
888
889 55. Grahl, S. Tat signal peptide recognition during protein maturation and export. doctoral
890 degree thesis, University of Dundee, Dundee, 2011.
891
892 56. Helle, L. *et al.* Vectors for improved Tet repressor-dependent gradual gene induction
893 or silencing in *Staphylococcus aureus*. *Microbiology* **157**, 3314-3323 (2011).
894
895 57. Corrigan, R.M. & Foster, T.J. An improved tetracycline-inducible expression vector for
896 *Staphylococcus aureus*. *Plasmid* **61**, 126-129 (2009).
897
898 58. Guzman, L.M., Belin, D., Carson, M.J. & Beckwith, J. Tight regulation, modulation, and
899 high-level expression by vectors containing the arabinose $P_{BAD}$ promoter. *J Bacteriol*
900 **177**, 4121-4130 (1995).
901
902 59. Jack, R.L. *et al.* Coordinating assembly and export of complex bacterial proteins.
903 *EMBO J* **23**, 3962-3972 (2004).
904
905 60. Fritsch, M.J. *et al.* Proteomic identification of novel secreted antibacterial toxins of the
906 *Serratia marcescens* type VI secretion system. *Mol Cell Proteomics* **12**, 2735-2749
907 (2013).
908
909 61. Hamilton, J.J. *et al.* A holin and an endopeptidase are essential for chitinolytic protein
910 secretion in *Serratia marcescens*. *J Cell Biol* **207**, 615-626 (2014).
911
912 62. Cianfanelli, F.R. *et al.* VgrG and PAAR Proteins Define Distinct Versions of a
913 Functional Type VI Secretion System. *PLoS Pathog* **12**, e1005735 (2016).
914

63. Trunk, K. *et al.* The type VI secretion system deploys antifungal effectors against microbial competitors. *Nat Microbiol* **3**, 920-931 (2018).

64. Cox, J. & Mann, M. MaxQuant enables high peptide identification rates, individualized p.p.b.-range mass accuracies and proteome-wide protein quantification. *Nat Biotechnol* **26**, 1367-1372 (2008).

65. Tyanova, S. *et al.* The Perseus computational platform for comprehensive analysis of (prote)omics data. *Nat. Methods* **13**, 731-740 (2016).

66. Vizcaino, J.A. *et al.* 2016 update of the PRIDE database and its related tools. *Nucleic Acids Res.* **44**, D447-456 (2016).

67. Keller, R., de Keyzer, J., Driessen, A.J. & Palmer, T. Co-operation between different targeting pathways during integration of a membrane protein. *J Cell Biol* **199**, 303-315 (2012).

68. Gotz, F., Ahrne, S. & Lindberg, M. Plasmid transfer and genetic recombination by protoplast fusion in staphylococci. *J Bacteriol* **145**, 74-81 (1981).

69. Miller, M. *et al. Staphylococcal* PknB as the first prokaryotic representative of the proline-directed kinases. *PLoS ONE* **5**, e9057 (2010).

70. Miyata, S.T., Unterweger, D., Rudko, S.P. & Pukatzki, S. Dual expression profile of type VI secretion system immunity genes protects pandemic *Vibrio cholerae*. *PLoS Pathog* **9**, e1003752 (2013).

71. Hall, C., Flores, M.V., Storm, T., Crosier, K. & Crosier, P. The zebrafish lysozyme C promoter drives myeloid-specific expression in transgenic fish. *BMC Dev Biol* **7**, 42 (2007).

72. Westerfield, M. *The zebrafish book. A guide for the laboratory use of zebrafish (Danio rerio).* 4th edn. University of Oregon: Eugene, 2000.

A

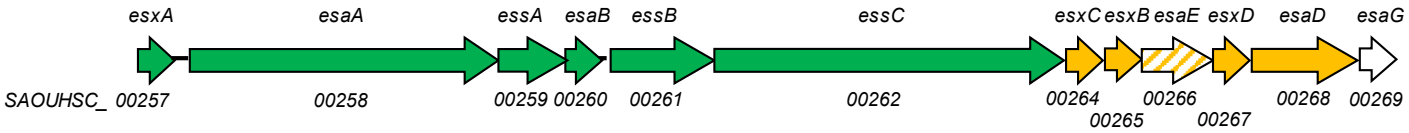


B

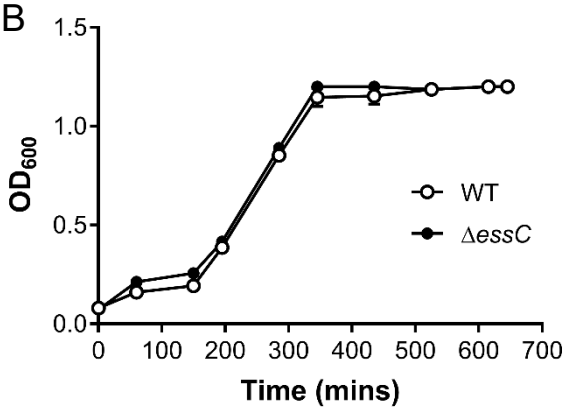


C

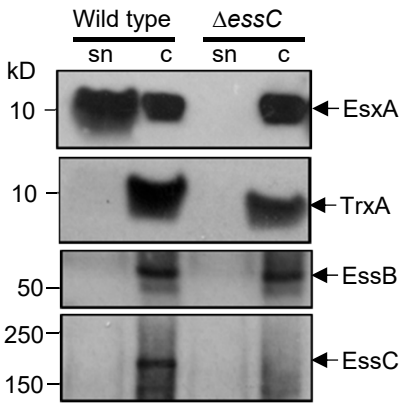


D

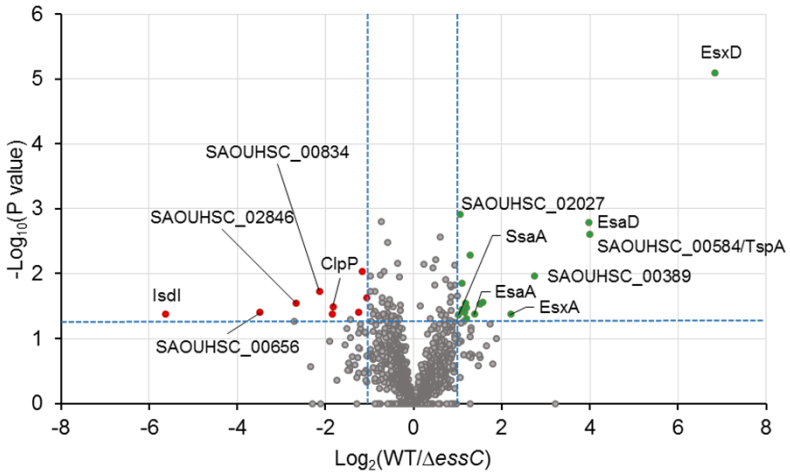


E

| Identifier | Protein name/description | Relative abundance WT/ΔessC | P-value | Unique peptides | Sequence coverage [%] |
|---|---|---|---|---|---|
| SAOUHSC_00267 | EsxD (T7 secreted substrate) | 113.6* | $8.00 \times 10^{-6}$ | 4 | 47.6 |
| SAOUHSC_00584 | (TspA) Uncharacterized LXG domain protein | 15.9 | $2.45 \times 10^{-3}$ | 16 | 44.3 |
| SAOUHSC_00268 | EsaD (T7 secreted nuclease) | 15.8 | $1.64 \times 10^{-3}$ | 24 | 44.5 |
| SAOUHSC_00389 | Uncharacterized. Predicted superantigen-like protein | 6.7* | 0.00109 | 2 | 25.6 |
| SAOUHSC_00257 | EsxA (Secreted T7 core component) | 4.6 | 0.00425 | 6 | 81.4 |
| SAOUHSC_00406 | Uncharacterized protein | 3.0 | 0.00272 | 10 | 31.7 |
| SAOUHSC_01342 | Nuclease SbcCD subunit C | 2.9 | 0.00291 | 7 | 9.7 |
| SAOUHSC_01949 | Intracellular serine protease, putative | 2.6 | 0.00421 | 7 | 20.8 |
| SAOUHSC_02028 | PhiETA ORF57-like protein | 2.4 | $5.21 \times 10^{-3}$ | 13 | 26.4 |
| SAOUHSC_01191 | 50S ribosomal protein L28 | 2.3 | 0.00498 | 3 | 24.2 |
| SAOUHSC_02695 | Uncharacterized protein with DUF4467/cystatin-like domain | 2.3 | 0.00337 | 5 | 31 |
| SAOUHSC_01180 | Uncharacterized protein | 2.3 | 0.00286 | 26 | 73.2 |
| SAOUHSC_00258 | EsaA (membrane-bound T7 core component) | 2.2 | 0.00397 | 71 | 59.4 |
| SAOUHSC_02448 | Uncharacterized protein with alpha/beta hydrolase fold | 2.1 | 0.00353 | 17 | 59.2 |
| SAOUHSC_02042 | Phi Mu50B-like protein | 2.1 | 0.00141 | 2 | 18.9 |
| SAOUHSC_02027 | SLT orf 129-like protein | 2.1 | $1.22 \times 10^{-3}$ | 4 | 56 |
| SAOUHSC_02883 | Staphylococcal secretory antigen SsaA | 2.0 | 0.00431 | 5 | 43.1 |

Fig 1

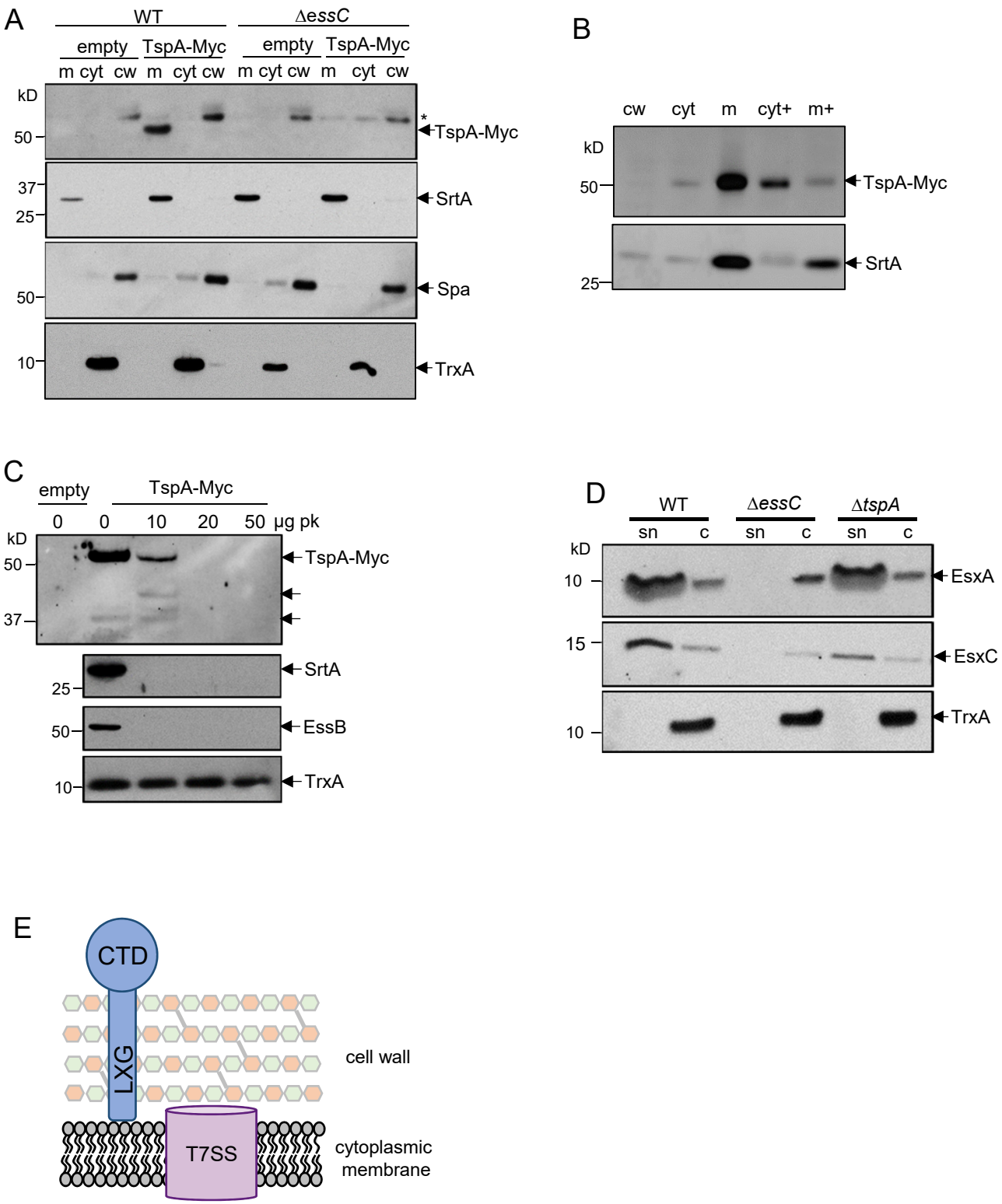
A
WT
ΔessC
empty
TspA-Myc
empty
TspA-Myc
m cyt cw m cyt cw m cyt cw m cyt cw
kD
50
37
25
50
10
*
TspA-Myc
SrtA
Spa
TrxA
B
cw cyt m cyt+ m+
kD
50
25
TspA-Myc
SrtA
C
empty
TspA-Myc
0 0 10 20 50 µg pk
kD
50
37
25
50
10
TspA-Myc
SrtA
EssB
TrxA
D
WT
ΔessC
ΔtspA
sn c sn c sn c
kD
10
15
10
EsxA
EsxC
TrxA
E
CTD
LXG
cell wall
T7SS
cytoplasmic membrane

Fig 2

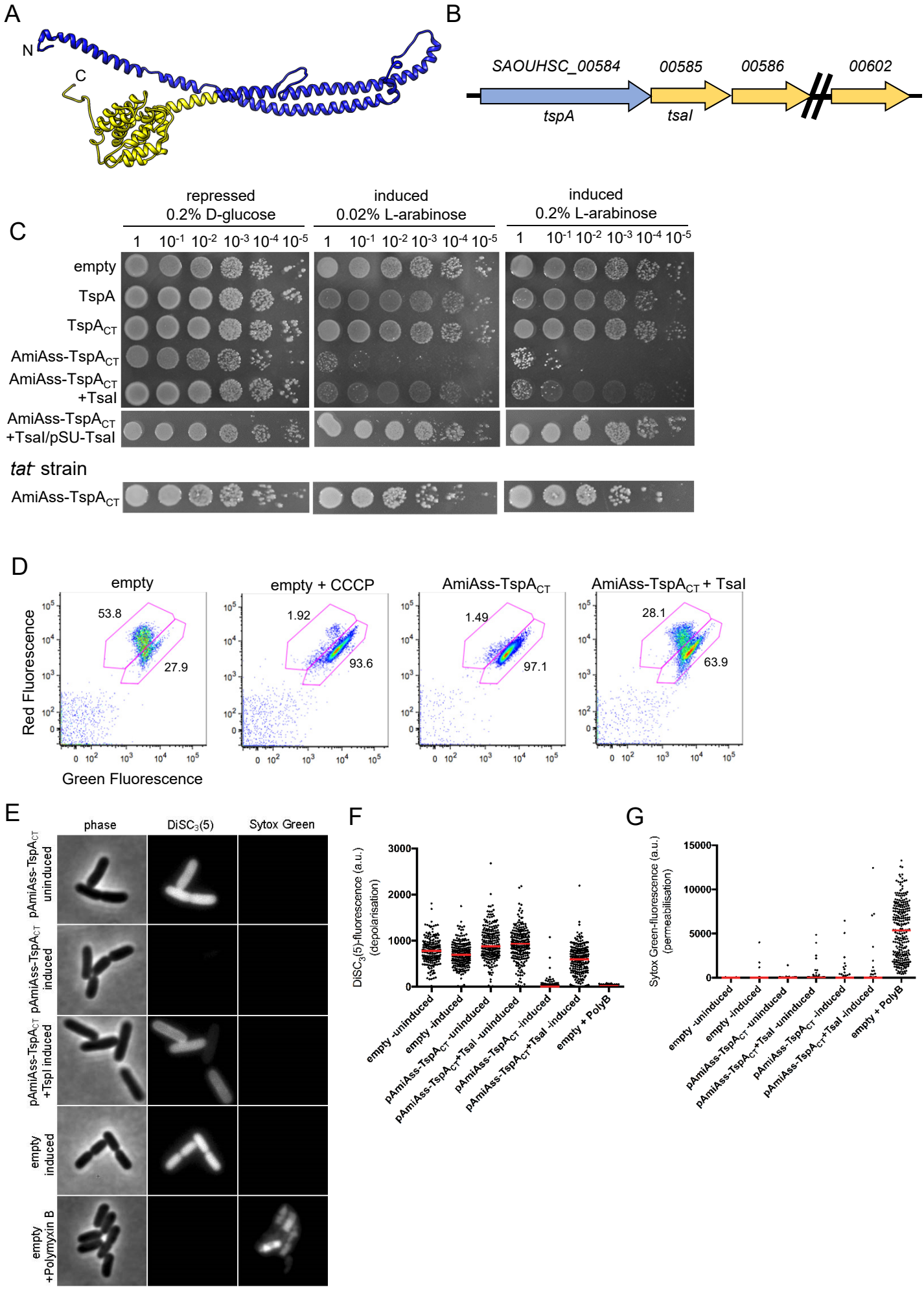
A
N
C
B
SAOUHSC_00584
00585
00586
00602
tspA
tsaI
C
repressed
0.2% D-glucose
induced
0.02% L-arabinose
induced
0.2% L-arabinose
1 10-1 10-2 10-3 10-4 10-5
empty
TspA
TspACT
AmiAss-TspACT
AmiAss-TspACT +TsaI
AmiAss-TspACT +TsaI/pSU-TsaI
tat- strain
AmiAss-TspACT
D
empty
empty + CCCP
AmiAss-TspACT
AmiAss-TspACT + TsaI
53.8
27.9
1.92
93.6
1.49
97.1
28.1
63.9
Red Fluorescence
Green Fluorescence
E
phase
DiSC3(5)
Sytox Green
pAmiAss-TspACT uninduced
pAmiAss-TspACT induced
pAmiAss-TspACT +TspI induced
empty induced
empty +Polymyxin B
F
DiSC3(5)-fluorescence (a.u.) (depolarisation)
empty -uninduced
empty -induced
pAmiAss-TspACT -uninduced
pAmiAss-TspACT+TsaI -uninduced
pAmiAss-TspACT -induced
pAmiAss-TspACT+TsaI -induced
empty + PolyB
G
Sytox Green-fluorescence (a.u.) (permeabilisation)

Fig 3

A

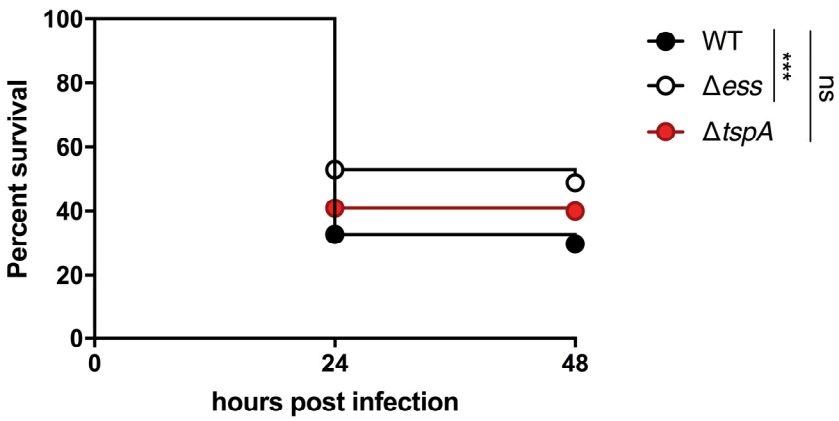
Percent survival
100
80
60
40
20
0
0
24
48
hours post infection
WT
Δess
ΔtspA
***
ns

B

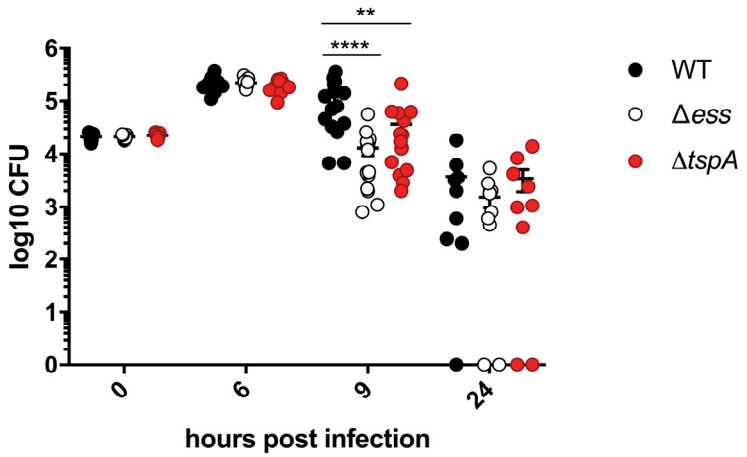
log10 CFU
6
5
4
3
2
1
0
0
6
9
24
hours post infection
**
****
WT
Δess
ΔtspA

C

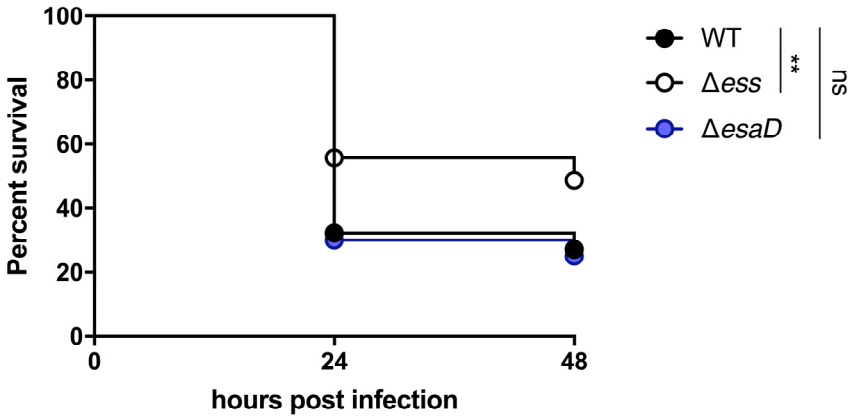
Percent survival
100
80
60
40
20
0
0
24
48
hours post infection
WT
Δess
ΔesaD
**
ns

D

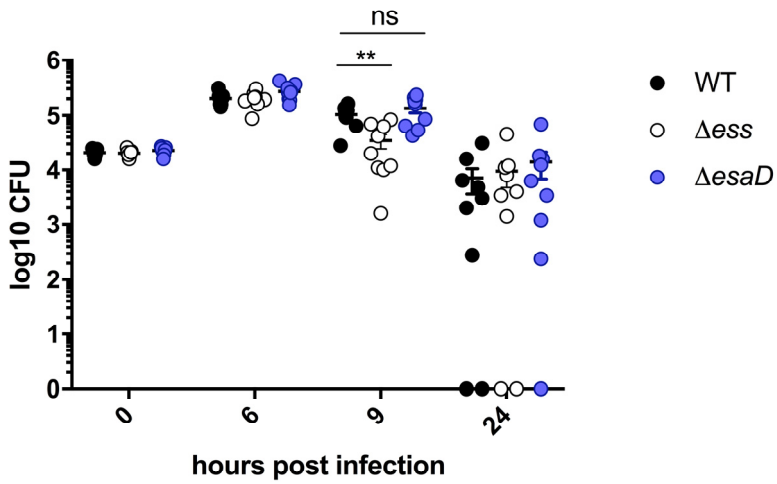
log10 CFU
6
5
4
3
2
1
0
0
6
9
24
hours post infection
ns
**
WT
Δess
ΔesaD

Fig 4

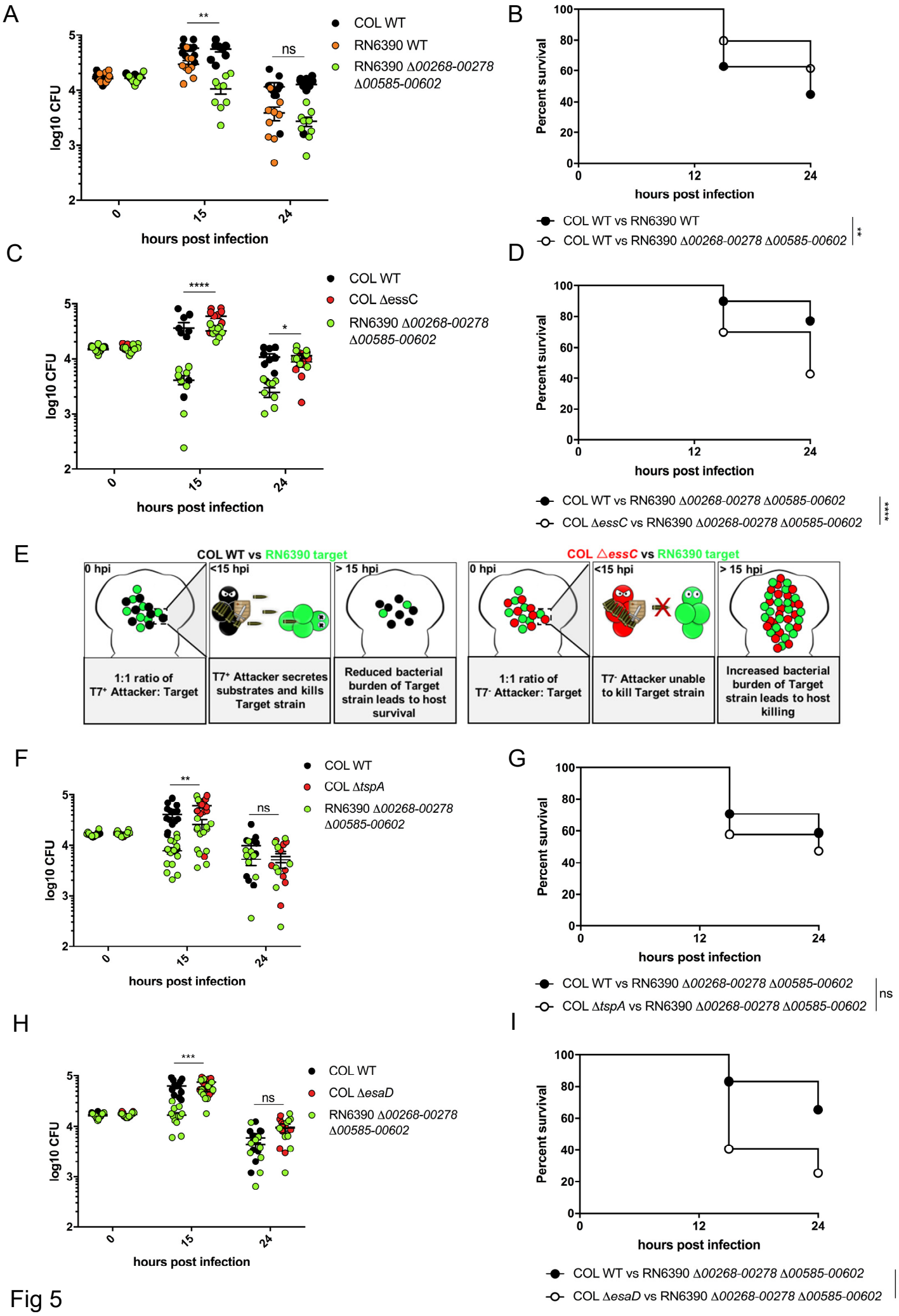
A
log10 CFU
hours post infection
COL WT
RN6390 WT
RN6390 Δ00268-00278 Δ00585-00602
**
ns
B
Percent survival
hours post infection
COL WT vs RN6390 WT
COL WT vs RN6390 Δ00268-00278 Δ00585-00602
**
C
log10 CFU
hours post infection
COL WT
COL ΔessC
RN6390 Δ00268-00278 Δ00585-00602
****
*
D
Percent survival
hours post infection
COL WT vs RN6390 Δ00268-00278 Δ00585-00602
COL ΔessC vs RN6390 Δ00268-00278 Δ00585-00602
****
E
COL WT vs RN6390 target
COL ΔessC vs RN6390 target
0 hpi
<15 hpi
> 15 hpi
1:1 ratio of T7+ Attacker: Target
T7+ Attacker secretes substrates and kills Target strain
Reduced bacterial burden of Target strain leads to host survival
1:1 ratio of T7- Attacker: Target
T7- Attacker unable to kill Target strain
Increased bacterial burden of Target strain leads to host killing
F
log10 CFU
hours post infection
COL WT
COL ΔtspA
RN6390 Δ00268-00278 Δ00585-00602
**
ns
G
Percent survival
hours post infection
COL WT vs RN6390 Δ00268-00278 Δ00585-00602
COL ΔtspA vs RN6390 Δ00268-00278 Δ00585-00602
ns
H
log10 CFU
hours post infection
COL WT
COL ΔesaD
RN6390 Δ00268-00278 Δ00585-00602
***
ns
I
Percent survival
hours post infection
COL WT vs RN6390 Δ00268-00278 Δ00585-00602
COL ΔesaD vs RN6390 Δ00268-00278 Δ00585-00602
****

Fig 5

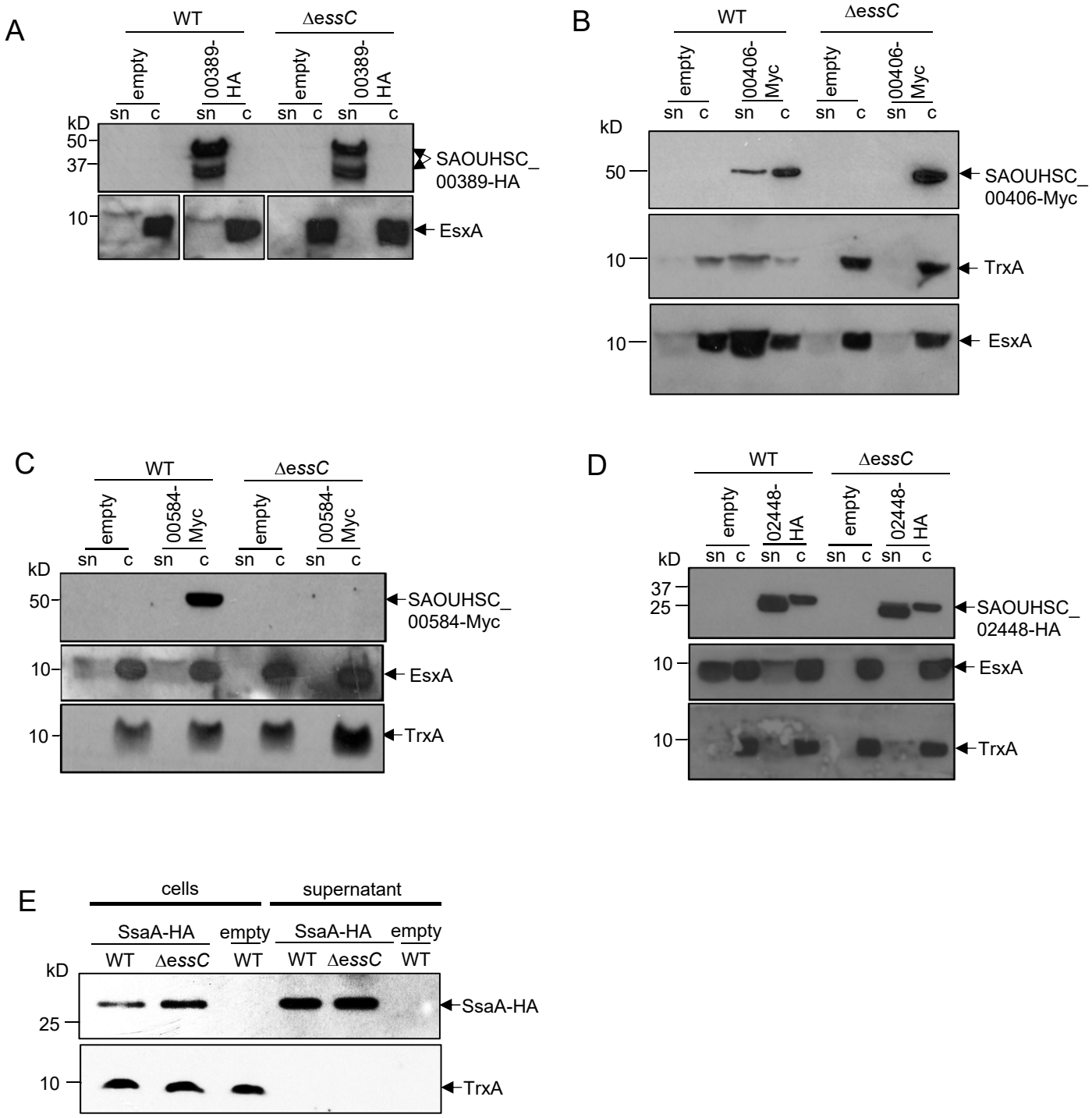
A
WT
ΔessC
empty
00389-HA
empty
00389-HA
sn c sn c sn c sn c
kD
50
37
10
SAOUHSC_ 00389-HA
EsxA
B
WT
ΔessC
empty
00406-Myc
empty
00406-Myc
sn c sn c sn c sn c
kD
50
10
10
SAOUHSC_ 00406-Myc
TrxA
EsxA
C
WT
ΔessC
empty
00584-Myc
empty
00584-Myc
sn c sn c sn c sn c
kD
50
10
10
SAOUHSC_ 00584-Myc
EsxA
TrxA
D
WT
ΔessC
empty
02448-HA
empty
02448-HA
sn c sn c sn c sn c
kD
37
25
10
10
SAOUHSC_ 02448-HA
EsxA
TrxA
E
cells
supernatant
SsaA-HA
empty
SsaA-HA
empty
WT ΔessC WT WT ΔessC WT
kD
25
10
SsaA-HA
TrxA

Fig S1

MSIDMYLDRSRNQASSVGNLSQTMNSNYDALEKAITQFINDDALKGKAYTSAKQFFSTVLIPLSTSMK
TLSDLTKQACDNFVSRYTSEVDSISLKESELEEDIRSLSQQITRYENLNNNLKKHASDNQQAISSNQQ
IIRTLGQQKHELEEKLRKLREFNQKSPEIFKEVEEFQKIVQQGLTQAQNFWNFSTNQFNIPSGKELDW
AKASHEKYLKVAMGKIEHKAEKETLNKADFAVIKAYAKEHPEDDIPKSILKYINDNKDSIKRDIGLDI
TSTLLEQDGINASKFGVFINTAGGVKGPAGPNSFVEVKRTSGNVFIENGSKFAKGGKYLGKGVAGVGF
GIGMYDDLANDDKTFGEALSHNGMTLAAGSAGTAVGAGLATFVLGSNPVGWVILAGLAMSTVFALGTD
LIYQNNIFGLKDKVDWVGHKIDNSIDVVKKTTEKSMDSVGNAVSEAKNIISNHINPMKWAW

Fig S2

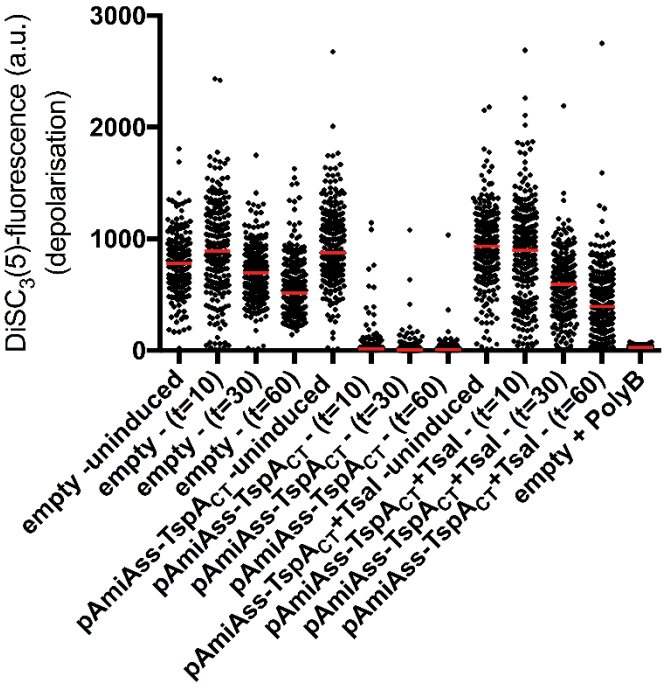
DiSC3(5)-fluorescence (a.u.)
(depolarisation)
3000
2000
1000
0
empty -uninduced
empty - (t=10)
empty - (t=30)
empty - (t=60)
pAmiAss-TspACT-uninduced
pAmiAss-TspACT - (t=10)
pAmiAss-TspACT - (t=30)
pAmiAss-TspACT - (t=60)
pAmiAss-TspACT+Tsal -uninduced
pAmiAss-TspACT+Tsal - (t=10)
pAmiAss-TspACT+Tsal - (t=30)
pAmiAss-TspACT+Tsal - (t=60)
empty + PolyB

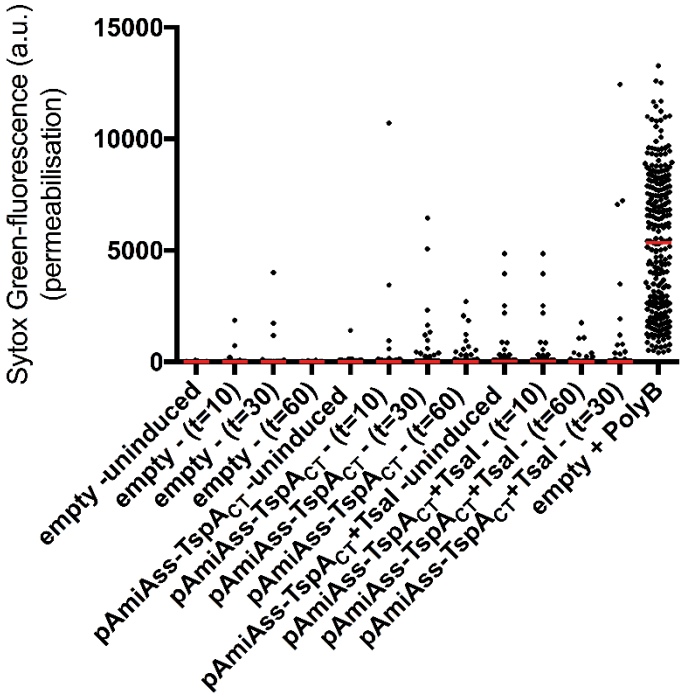
Sytox Green-fluorescence (a.u.)
(permeabilisation)
15000
10000
5000
0
empty -uninduced
empty - (t=10)
empty - (t=30)
empty - (t=60)
pAmiAss-TspACT-uninduced
pAmiAss-TspACT - (t=10)
pAmiAss-TspACT - (t=30)
pAmiAss-TspACT - (t=60)
pAmiAss-TspACT+Tsal -uninduced
pAmiAss-TspACT+Tsal - (t=10)
pAmiAss-TspACT+Tsal - (t=30)
pAmiAss-TspACT+Tsal - (t=60)
empty + PolyB

Fig S3

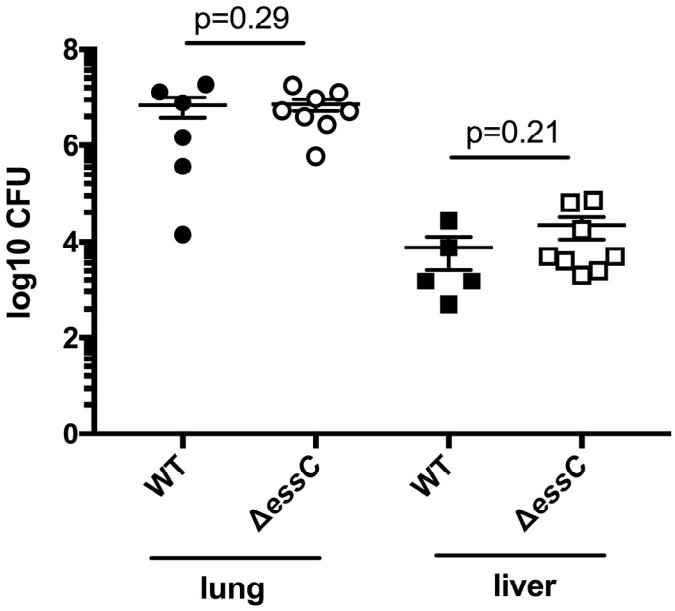


Fig S4

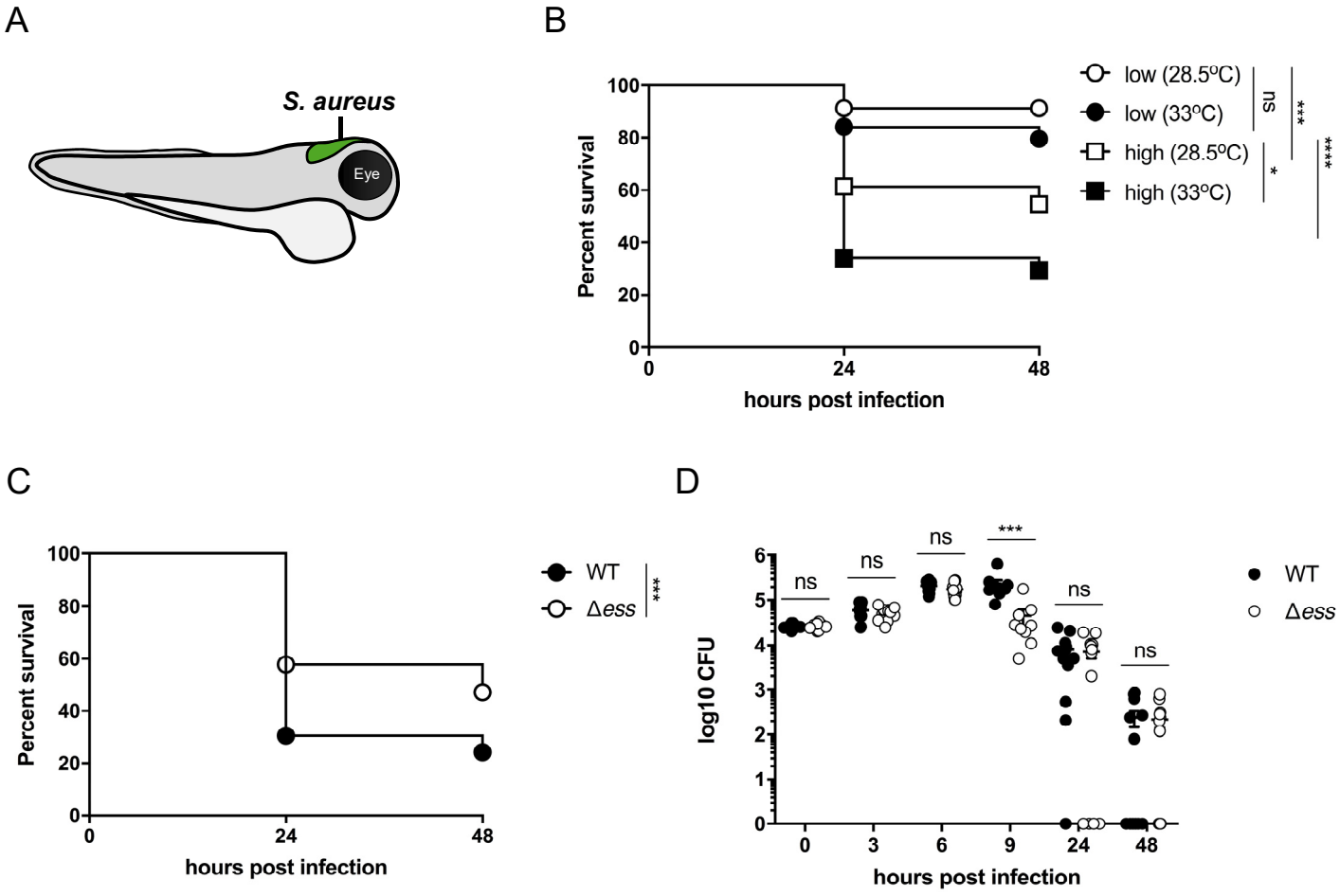
A
S. aureus
Eye
B
Percent survival
hours post infection
low (28.5ºC)
low (33ºC)
high (28.5ºC)
high (33ºC)
ns
***
*
****
C
Percent survival
hours post infection
WT
Δess
***
D
log10 CFU
hours post infection
ns
***
WT
Δess

Fig S5

A

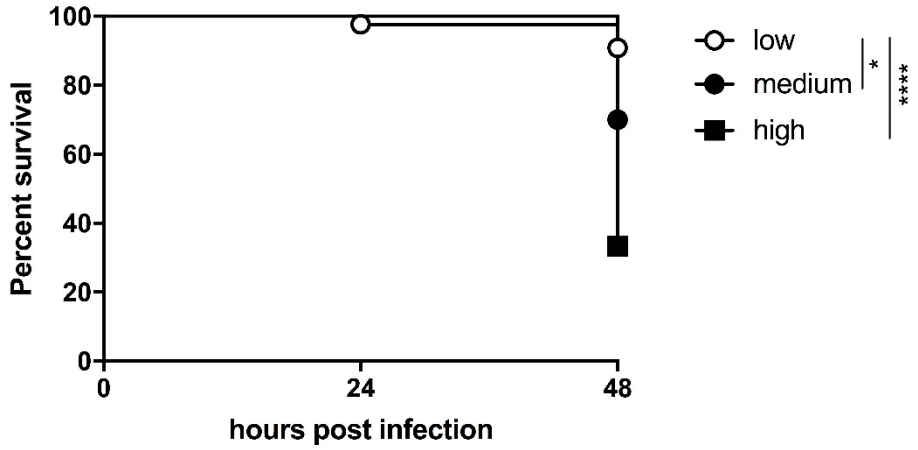
100
80
60
40
20
0
Percent survival
0
24
48
hours post infection
low
medium
high
*
****

B

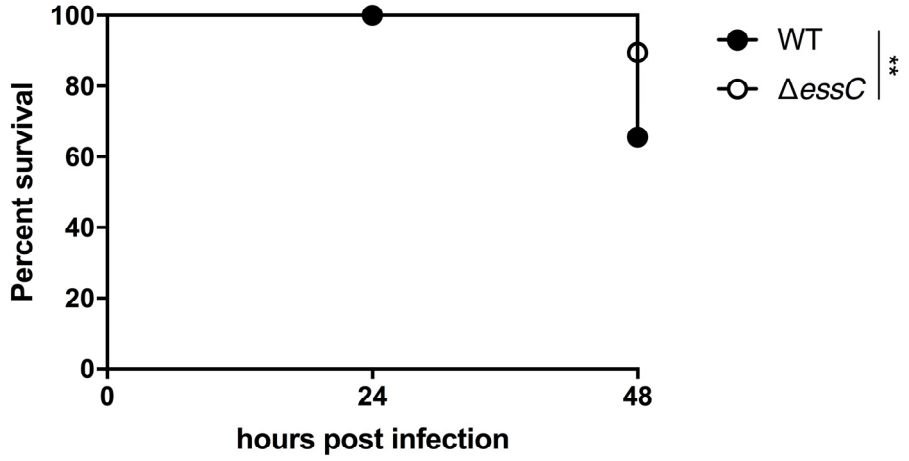
100
80
60
40
20
0
Percent survival
0
24
48
hours post infection
WT
ΔessC
**

C

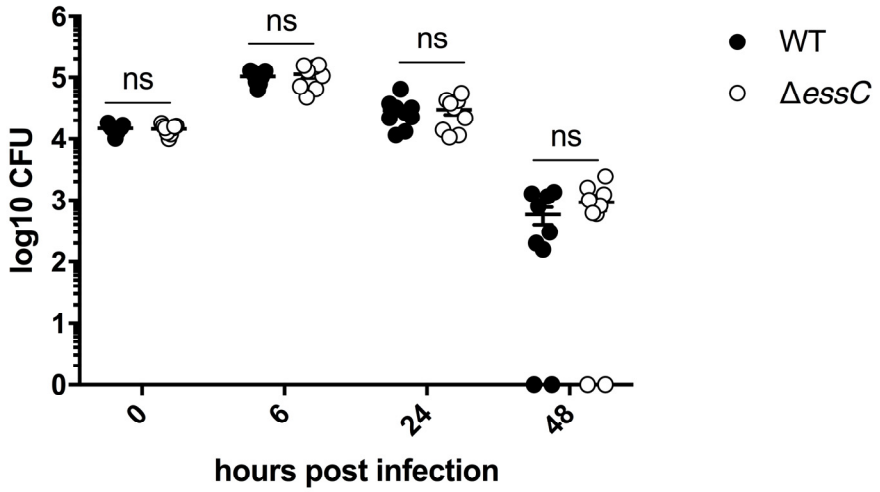
6
5
4
3
2
1
0
log10 CFU
ns
ns
ns
ns
0
6
24
48
hours post infection
WT
ΔessC

Fig S6

```
YP_499151.1        1 MSIDMYLDRSRNQASSVGNLSQTMNSNYDALEKAITQFINDDALKGKAYTSAKQFFSTVLIPLSTSMKTLSDLTKQACDNFVSRYTSEVDSISLKESELEEDIRSLSQQITRYENLNNNL
WP_000020789.1     1 MSIDMYLDRSRNQASSVGNLSQTMNSNYDALEKAITQFINDDALKGKAYTSAKQFFSAVLIPLSTSMKTLSDLTKQACDNFVSRYTSEVDSISLKESELEEDIRSLSQQITRYENLNNNL
WP_061738882.1     1 MSIDMYLDRSRNQASSVGNLSQTMNSNYDALEKAITQFINDDALKGKAYTSAKQFFSTVLIPLSTSMKTLSDLTKQACDNFVSRYTSEVDSISLKESELEEDIRSLSQQITRYENLTNNL
WP_020977030.1     1 MSIDMYLDRSRNQASSVGDLSQTMNSNYDALEKAITQFINDDALKGKAYTSAKQFFSTVLIPLSTSMKTLSDLTKQACDNFVSRYTSEVDSISLKESELEEDIRSLSQQITRYENLNNNL
WP_000020798.1     1 MSIDMYLDRSRNQASSVGNLSQTMNSNYDALEKAITQFINDDALKGKAYTSAKQFFSTVLIPLSTSMKTLSDLTKQACDNFVSRYTSEVDSISLKESELEEDIRSLSQQITRYENLNNNL
WP_054189160.1     1 MSIDMYLDRSRNQASSVGNLSQSMNSNYDALEKAITQFINDDALKGKAYTSAKQFFSTVLIPLSTSMKTLSDLTKQACDNFVSRYTSEVDSISLKESELEEDIRSLSQQITRYENLNNNL
WP_047530207.1     1 MSIDMYLDRSRNQASSVGNLSQSMNSNYDALEKAITQFINDDALKGKAYTSAKQFFSTVLIPLSTSMKTLSDLTKQACDNFVSRYTSEVDSISLKESELEEDIRSLSQQITRYENLNNNL
WP_000020802.1     1 MSIDMYLDRSRNQASSVGNLSQTMNSNYDALEKAITQFINDDALKGKAYTSAKQFFSTVLIPLSTSMKTLSDLTKQACDNFVSRYTSEVDSISLKESELEEDIRSLSQQITRYENLNNNL
WP_000020810.1     1 MSIDMYLDRSRNQASSVGNLSQTMNSNYDALEKAITQFINDDALKGKAYTSAKQFFSTVLIPLSTSMKTLSDLTKQACDNFVSRYTSEVDSISLKESELEEDIRSLSQQITRYENLNNNL

YP_499151.1      121 KKHASDNQQAISSNQQIIRTLGQQKHELEEKLRKLREFNQKSPEIFKEVEEFQKIVQQGLTQAQNFWNFSTNQFNIPSGKELDWAKASHEKYLKVAMGKIEHKAEKETLNKADFAVIKAY
WP_000020789.1   121 KKHASDNQQAISSNQQIIRTLGQQKHELEEKLRKLREFNQKSPEIFKEVEEFQKIVQQGLTQAQNFWNFSTNQFNIPSGKELDWAKASHEKYLKVAMGKIEHKAEKETLNKADFAVLKAY
WP_061738882.1   121 KKHASDNQQAISSNQQIIQTLGQQKHELEEKLRKLREFNQKSPEIFKEVEEFQKIVQQGLTQAQNFWNFSTNQFNIPSGKELDWAKASHEKYLKVAMGKIEHKAEKETLNKADFAVIKAY
WP_020977030.1   121 KKHASDNQQAISSNQQIIQTLGQQKHELEEKLRKLREFNQKSPEIFKEVEEFQKIVQQGLTQTQNFWNFSTNQFNIPSGKELDWAKASHEKYLKVAMGKIEQKAEKETLNKADFAVIKAY
WP_000020798.1   121 KKHASDNQQAISSNQQIIRTLGQQKHELEEKLRKLREFNQKSPEIFKEVEEFQKIVQQGLTQAQNFWNFSTNQFNIPSGKELDWAKASHEKYLEVAMGKIEHKAEKETLNKADFAVIKAY
WP_054189160.1   121 KKHASDNQQAISSNQQIIQTLGQQKHELEEKLRKLREFNQKSPEIFKEVEEFQKIVQQGLTQAQNFWNFSTNQFNIPSGKELDWAKASHEKYLKVAMGKIEHKAEKETLNKADFAVIKAY
WP_047530207.1   121 KKHASDNQQAISSNQQIIQTLGQQKHELEEKLRKLREFNQKSPEIFKEVEEFQKIVQQGLTQAQNFWNFSTNQFNIPSGKELDWAKASHEKYLEVAMGKIEHKAEKETLNKADFAVIKAY
WP_000020802.1   121 KKHASDNQQAISSNQQIIRTLGQQKHELEEKLRKLREFNQKSPEIFKEVEEFQKIVQQGLTQAQNFWNFSTNQFNIPSGKELDWAKASHEKYLKVAMGKIEHKAEKETLNKADFAVIKAY
WP_000020810.1   121 KKHASDNQQAISSNQQIIRTLGQQKHELEEKLRKLREFNQKSPEIFKEVEEFQKIVQQGLTQAQNFWNFSTNQFNIPSGKELDWAKASHEKYLKVAMGKIEQKAEKETLNKADFAVIKAY

YP_499151.1      241 AKEHPEDDIPKSILKYINDNKDSIKRDIGLDITSTLLEQDGINASKFGVFINTAGGVKGPAGPNSFVEVKRTSGNVFIENGSKFAKGGKYLGKGVAGVGFGIGMYDDLANDDKTFGEALS
WP_000020789.1   241 AKEHPEDDIPKSIMKYINDNKDSIKRDIGLDITSTLLEQGGINASKFGVFINTAGGVKGSAGPNSFVEVKRTSGNVFIENGSKFAKGGKYLGKGVAGVGFAIGMYDDMANDDKTVGEALS
WP_061738882.1   241 AKEHPEDDIPKSIMKYINDNKDSIKRDIGLDITSTLLEQGGINASKFGVFINTAGGVKGPAGPNSFVEVKRTSGNVFIENGSKFAKGGKYLGKGVAGVGFGIGMYDDLANDDKTFGEALS
WP_020977030.1   241 AKEHPEDDIPKSIMKYINDNKDSIKRDIGLDITSTLLEQGGINASKFGVFINTAGGVKGPAGPNSFVEVKRTSGNVFIENGSKFAKGGKYLGKGVAGVGFGIGMYDDLANDDKTFGEALS
WP_000020798.1   241 AKEHPEDDIPKSIMKYINDNKDSIKRDIGLDITSTLLEQGGINASKFGVFINTAGGVKGPAGPNSFVEVKRTSGNVFIENGSKFAKGGKYLGKGVAGVGFAIGMYDDMANDDKTVGEALS
WP_054189160.1   241 AKEHPEDDIPKSIMKYINDNKDSIKRDIGLDITSTLLEQGGINASKFGVFINTAGGVKGPAGPNSFVEVKRTSGNVFIENGSKFAKGGKYLGKGVAGVGFGIGMYDDMANDDKTVGEALS
WP_047530207.1   241 AKEHPEDDIPKSIMKYINDNKDSIKRDIGLDITSTLLEQGGINASKFGVFINTAGGVKGPAGPNSFVEVKRTSGNVFIENGSKFAKGGKYLGKGVAGVGFGIGMYDDLANDDKTVGEALS
WP_000020802.1   241 AKEHPEDDIPKSIMKYINDNKDSIKRDIGLDITSTLLEQGGINASKFGVFINTADGVKGPAGPNSFVEVKRTSGNVFIENGSKFAKGGKYLGKGVAGVGFGIGMYDDLANDDKTFGEALS
WP_000020810.1   241 AKEHPEDDIPKSIMKYINDNKDSIKRDIGLDITSTLLEQGGINASKFGVFINTAGGVKGPAGPNSFVEVKRTSGNVFIENGSKFAKGGKYLGKGVAGVGFGIGMYDDMANDDKTVGEALS

YP_499151.1      361 HNGMTLAAGSAGTAVGAGLAAFVLGSNPVGWVLLAGLAMSTVFALGTDLLIYQNNIFGLKDKVDWVGHKIDNSIDVVKKTTEKSMDSVGNAVSEAKNIISNHINPMKWAW
WP_000020789.1   361 HNGMTLAAGVGT---TALITIFLGS-NPVGIAVLAGFALGCLATKGADWAYQNNWKGIKDKTDWVGHKIDDGIDVVKKSTEKAVDSVGNVVGEATKSISDHINPMKWSW
WP_061738882.1   361 HNGMTLAAGSVAAFGVAALVSNPVG-----WAVVGILTAGLLGSIASDVLIYQNNYFGIKDKVDWAGHKIDEGIDAVNKTAEKAVDSVGNTIGDATKSISNHINPMKWSW
WP_020977030.1   361 HNALTTGIGTGAG---IAITAALAT-NPVGWTVLAGFAVGTLFTFITDWAYQNNIAGIKDKADWVGHKIDDGIDVAKKSTEKALDSVGNVVGQATKSISDHINPMKWSW
WP_000020798.1   361 HNGMTLAAGSAMGTIVSVGTTMLAS-NPVGWAVLGGFAAATGFAIAADWAYENNLWGLKDETDWVGHKIDDGIDVVKKSTEKAVDSVEKAVGEATKSISNHINPMKWSW
WP_054189160.1   361 HNGMTLAAG----VGTTAAITFFLSSNPVGWATVGILSAAFYISMITDWAYQNNKAGIKDKVDWVGHKIDDGIDAVKNTTEKAVDSVGTVVGEATNNISDHINPMKWAW
WP_047530207.1   361 HNGMTLAAGSVAGASMSAGITLLAS-NPVGWAVLGGFAVATGITIAADWAYENNMWGLKDKTDWVGHKIDDGIDVVKNSTKKALDSVESAVGEATKSISKHINPMKWSW
WP_000020802.1   361 HNGMTLAAGSGAGAVVTVGASILLGSNPVGWAVIGGFVAGTIVSKLADWAYQSNWNGIKDKTDWVGHKIDDSIDVVKKSTEKAVDSVG----EATKSISNHLNPMKWSW
WP_000020810.1   361 HNALTTGIGIGAGAGMTATIALFAS-NPVGWAVIGGFVFGSVSTVLVDWAYQNNKAGIKDKADWVGHKLDDGIDVVKKSTEKAVDSVG----EATKSISNHLNPMKWSW
```

Fig S7